Submitted to *Operations Research*
manuscript (Please, provide the manuscript number!)

Transmission capacity allocation in zonal electricity markets

Ignacio Aravena
Lawrence Livermore National Laboratory, Livermore, CA, USA
aravenasolis1@llnl.gov

Quentin Lété, Anthony Papavasiliou, Yves Smeers
CORE, Université catholique de Louvain, Louvain-la-Neuve, Belgium
{quentin.lete, anthony.papavasiliou, yves.smeers}@uclouvain.be

We propose a novel framework for modeling zonal electricity markets, based on projecting the constraints of the nodal network onto the space of the zonal aggregation of the network. The framework avoids circular definitions and discretionary parameters, which are recurrent in the implementation and study of zonal markets. Using this framework, we model and analyze two zonal market designs currently present in Europe: flow-based market coupling (FBMC) and available-transfer-capacity market coupling (ATCMC). We develop cutting-plane algorithms for simulating FBMC and ATCMC while accounting for the robustness of imports/exports to single element failures, and we conduct numerical simulations of FBMC and ATCMC on a realistic instance of the Central Western European system under the equivalent of 100 years of operating conditions. We find that FBMC and ATCMC are unable to anticipate the congestion of branches interconnecting zones and branches within zones, and that both zonal designs achieve similar overall cost efficiencies (0.01% difference), while a nodal market design largely outperforms both of them (5.09% better than FBMC). These findings raise the question of whether it is worth for more European countries to switch from ATCMC to FBMC, instead of advancing directly towards a nodal market design.

1. Introduction

Zonal electricity markets schedule production and consumption in power systems using a simplified zonal representation of the underlying nodal electrical network. The zonal aggregation of the grid

allows market participants to trade freely within each zone and to export/import energy to/from other zones up to certain technical limitations. Two approaches toward zonal market design are the focus of this paper, both of which currently coexist in the European electricity market:

1. imposing limitations on the cross-border exchanges between pairs of neighboring zones, and
2. imposing limitations on the configuration of net positions (i.e. exports − imports) of zones.

The first approach is known as Available-Transfer-Capacity Market Coupling (ATCMC) (APX Group et al. 2010). Available transfer capacity (ATC) refers to the capacity of the interconnectors between pairs of zones. The second approach is known as Flow-Based Market Coupling (FBMC) (50Hertz et al. 2017). The term "flow-based" (FB) refers to the fact that FBMC mimics, at a zonal level, how electricity flows through the grid.

In FBMC, the export/import capacities of each zone are allocated implicitly, potentially capturing inter-dependencies between cross-border exchanges. Such inter-dependencies are ignored in ATCMC. Additionally, FBMC can handle a larger variety of constraints on inter-zonal exchanges than ATCMC, thereby allowing Transmission System Operators (TSOs) to include transmission constraints in a more transparent and explicit manner for day-ahead market clearing. Consequently, under FBMC, TSOs may not need to consider large security margins on cross-border exchanges.

The expected benefits of FBMC rendered it as the preferred method for linking markets in the European Union. This decision was ratified by Regulation (EC) 2015/1222 and it led to the implementation of FBMC in the Central Western European (CWE) system, comprising Austria, Belgium, France, Germany, Luxembourg and the Netherlands, in May 2015.

Despite their differences, FBMC and ATCMC are both zonal electricity markets and, as such, they can only approximate the inter- and intra-zonal power flows of the real grid to a limited extent. This often causes market-clearing schedules that would result in overloaded transmission equipment under both FBMC and ATCMC. Congestion management measures are required after the clearing of the electricity market, in order to operate the system within its security limits in real time. The cost of these remedial measures can be very important, however it is commonly ignored in market

analyses. For instance, the parallel run between FBMC and ATCMC for the CWE (Amprion et al. 2015) found potential welfare gains of FBMC over ATCMC in the order of 95 M€ for 2013 while ignoring congestion management costs. These costs will amount to 945 M€ in 2015, the first year of operations under FBMC (ENTSO-E 2018). Therefore, by virtue of the magnitude of congestion management costs, the effect of these remedial actions could have affected the conclusions of the parallel run. Our aim, in this paper, is to overcome this and other common simplifications in the analysis of zonal markets by the development of models and algorithms capable of quantifying more accurately for the overall performance of different market designs, and allowing for comprehensive policy analyses.

1.1. Historical context

The European zonal electricity market directly inherited some of its major characteristics from the Nordic system (Norway, Sweden, Finland and Denmark). Both are based on a decomposition of the market into zones connected by aggregated representations of the lines of the network. The decomposition into zones first reflected national borders. The day-ahead market is a pure energy market run by a Power Exchange (PX), which is seen as the spot market, i.e. the last stage at which electricity is traded and according to which financial instruments are settled. The inevitable deviations between the day ahead and real time are treated by a special mechanism, initially run by national TSOs, that was only progressively integrated among them. Notwithstanding the integration of the energy market through a single PX, the management of the grid remains zonal. Redispatching is the main tool for dealing with congestion management in the Nordic system, but TSOs can also rely on the so-called "market splitting" to deal with intra-zonal congestion. This property was only systematically used by Norway but the EU competition authorities forced it on Sweden when the latter had difficulties managing congestion on a line to Denmark.

Other regions of the world have also implemented zonal markets. Australia is a case in point that one might want to compare to Europe insofar as the markets of the different States each form an area connected to the neighboring States by transport capacities. The zones are fixed

and determined by the State borders. Zonal markets also flourished in the United States (US) but soon gave way to nodal organizations. Peco, in Pennsylvania, was the first example of a zonal market: it was created in 1997 but collapsed after a year due to dispatching difficulties. The zonal system was one of the causes of the meltdown of the first California restructured market, which was subsequently replaced by a nodal market. Finally, ERCOT was the last attempt to install a zonal market in the US. Here, too, redispatching costs exploded compared to what was initially planned and ERCOT moved to a nodal model. Other restructured US systems immediately adopted the nodal framework.

The first trilateral version of the European market, coupling Belgium, France and the Netherlands, came live in November 2006 (APX Group et al. 2006) as a zonal system. This was possibly inspired by the Nordic experience and the careful mix of integration and remaining national identities. It has since developed to encompass the whole European continent, including the Nordic countries. However, the European zonal system did not resort to market splitting (except in the Nordic countries) but to a construction of "cross-border" capacities initally exposed in Regulation (EC) 2003/1228. The zones correspond to Member States (which can be as large areas as France and Germany, or as small as Belgium) and are thus based on a political configuration rather than a technical or economical analysis. Congestion is fully managed by redispatch. While the zonal system is enshrined in legislation, including Regulation (EC) 2003/1228, Regulation (EC) 2009/714, Regulation (EC) 2015/1222, one cannot exclude that the evolution may end up being more in line with what happened in the US. The reasons are technical. Well before restructuring, a common Nordic argument was that the Nordic transmission system had been designed for north-south transport (at the time Danish coal in the south and hydro in the north). The argument remains valid today but in a different form (Danish renewable power in the south and storage in the north). Unscheduled flows were thus not a main issue, given the largely radial grid structure. But neither the EU grid nor the US system were designed in such a radial fashion, with the consequence that unscheduled flows and congestion may turn out to be more important. Also, while the Nordic system exploited

zone splitting effectively in Norway in order to relieve the recourse to redispatching, the EU has so far always resisted resorting to smaller zones that could help when a single price zone contains congested "critical infrastructure". For instance, the recent bidding zone review performed by the European system operators recognized that the current configuration is inefficient, however the review failed to suggest recommendations for improving the bidding zone delimitation (ENTSO-E 2018, ACER 2019). Recalling the ERCOT experience when redispatching costs had been dismissed as irrelevant before they blew up a few years later, one can only note that these costs that were deemed to remain below 45 M€/year in Germany (2007, maximum prior to market coupling) now (2017) amount to 1 161 M€/year in that country (ENTSO-E 2018). Finally, it is worth mentioning that, apart from these efficiency effects, a zonal market followed by redispatching introduces cross-subsidies from consumers to generators and between Member States.

The models presented in this paper are intended to provide an instrument to understand the possible evolution of the zonal system. These models avoid simplifying assumptions often made in economic analyses and aim at being as realistic as possible in their encompassing of current and future legal obligations. The day-ahead market follows the organization described in Regulation (EC) 2009/714. Real-time operation, which is only currently defined in Regulation (EC) 2015/1222 and Regulation (EU) 2017/2195 stating legal objectives, assumes that these objectives are effectively realized. The price to pay for this lack of simplification is computational, both in terms of algorithmic tools as well as machine resources.

A European model can only be idiosyncratic because of its peculiar institutions. But with its coverage of 989 GW (ENTSO-E 2017), and about 500 million consumers (Eurostat 2018), the European market is significantly larger than all the restructured US markets (CAISO 60 GW, ERCOT 75 GW (FERC 2018)) and also than the largest US RTOs like PJM (166 GW (FERC 2018)) and MISO (174 GW (FERC 2018)). It can also be noted that the current European market organization introduces systematic discrepancies between the day-ahead and real-time representations of the system that are much deeper than the differences present in nodal market organizations,

which have been affecting some of the essential tools of US markets such as Virtual Trading. The methodology adopted here can be, if not directly transposed, at least adapted to examine the impact of phenomena such as the effect of unit commitment or transmission switching decisions on prices (Hogan 2016), which interrupt the normal mechanism of arbitrage between day ahead and real time in US markets.

1.2. Literature review

Owing to political and institutional constraints, the EU market carries a legacy market design which is characterized by a geographical and functional segmentation of short-term operations that are interdependent, and that can and should be co-optimized. The most notable consequences of this legacy market design are (i) the separation of reserve and energy clearing in day-ahead markets, (ii) the absence of a real-time market for reserve capacity, (iii) the reduced coordination of TSOs across geographic borders in real time, (iv) the artificial segmentation of real-time operations into congestion management and balancing, and (v) zonal pricing in the day ahead. There are numerous short-term and long-term inefficiencies and price formation barriers that result from this segmentation (Papavasiliou et al. 2019). These inefficiencies are becoming increasingly difficult to handle in a regime of large-scale renewable energy and distributed resource integration, which commands improved spatio-temporal coordination at the transmission and distribution level.

The separation of reserve and energy clearing in the day ahead impedes the accurate formation of forward reserve prices, since balancing service providers need to anticipate energy prices which dictate their opportunity cost for offering reserve, a function which is performed automatically in co-optimization. The absence of a real-time market for reserve capacity undermines the creation of a favorable environment for investing in operating reserve capacity, since it becomes extremely challenging to value reserve accurately based on real-time scarcity. Reduced real-time coordination makes it challenging for zones to share low-cost renewable resources across borders, when this supply becomes unexpectedly available in real time. The artificial segmentation of congestion management and balancing in real time is likely to result in conservative allocation of transmission

capacity in the emerging EU balancing platforms (PICASSO and MARI) in order to avoid security violations in real time. Zonal pricing in day-ahead operations results in inefficient commitment decisions of inflexible resources. The present paper does not aim at quantifying all of these effects simultaneously. Instead, the goal is to isolate the effect of zonal pricing on inefficient day-ahead unit commitment (item (v)). We therefore focus the literature review and model on this specific topic, and refer the reader to Papavasiliou et al. (2019) for a broader discussion and comparison of the impact of the aforementioned legacy market design features on short and long-term efficiency.

ATCMC has been the standard zonal electricity market model analyzed in the literature because of its past presence in US electricity markets and its current presence in European electricity markets. Studies using small examples and realistic systems, under various assumptions and modeling choices, have all concluded that the performance of ATCMC is significantly worse than that of a nodal system (see Aravena and Papavasiliou (2017) and references therein for a survey), even in the case where ATCs can be optimized so as to reduce real operation costs (Jensen et al. 2017).

Academic studies on FBMC, on the other hand, are scarce as FBMC is a relatively new capacity allocation methodology. Early studies were performed before the *go-live* of FBMC at the CWE. Waniek et al. (2010) study the day-ahead market performance and the accuracy of power flow approximations of ATCMC, FBMC and the nodal design. For ATCMC and FBMC, the authors disaggregate zonal injections into nodal injections in proportion to the injections in a base case (similar to the procedure followed by RTE, see 50Hertz et al. (2017)). The factors that are used for disaggregating zonal injections into nodal injections are know as Generation Shift Keys (GSKs) in the literature. The study finds that FBMC outperforms ATCMC in terms of both performance and accuracy, while the nodal design exhibits superior performance relative to both FBMC and ATCMC. Following the *go-live*, in an effort towards understanding the new capacity allocation mechanism, Van den Bergh et al. (2016) summarize the concepts and methodology used in FBMC.

Significant attention has been dedicated towards studying how discretionary parameters determined by TSOs affect the day-ahead outcome of FBMC. Marien et al. (2013) study the effect of

the configuration of bidding zones, and the determination of Flow Reliability Margins[1] and GSKs on exchanges and prices. The authors find that different choices for these parameters for the same system can lead to very different market outcomes. In the same vein, Dierstein (2017) analyses different strategies used by CWE TSOs to compute GSKs and how they affect the outcome of FBMC and congestion management for cross-border lines. The author finds that dynamic GSK strategies (i.e. where GSKs vary from one hour to the next) outperform static GSK strategies, the latter being currently used by all TSOs except RTE.

1.3. Contributions and paper organization

The contributions of the present paper are threefold. In terms of modeling, we propose a framework for modeling zonal electricity markets that avoids the discretionary parameters and circular definitions (i.e. definitions of parameters that depend on a base case) present in the current practice and in the literature. This is achieved in the proposed FBMC and ATCMC models by projecting the actual network constraints onto the space of zonal net positions and cross-border exchanges, respectively. The computational contribution of the paper is the development of cutting-plane algorithms for clearing the day-ahead market under each policy, while endogenously enforcing robustness of the import/export decisions against single-element contingencies (i.e. satisfying the N-1 security criterion, see 50Hertz et al. (2017), APX Group et al. (2010), RTE (2006)). The N-1 security criterion is an essential attribute that needs to be accounted for in the modeling of the European day-ahead market. The resulting clearing problems correspond to adjustable robust optimization problems (Ben-Tal et al. 2009). The policy contribution of the paper is the detailed simulation of a realistic-scale instance of the CWE system (Aravena and Papavasiliou 2017) against detailed models of the nodal design, FBMC and ATCMC. These simulations account for the clearing of energy and reserves, renewable supply forecasts errors and the outage of components, the pricing of non-convex operating costs and constraints, and the two-stage nature of market operations whereby day-ahead market clearing is followed by congestion management and balancing. Numerical results over the equivalent of 100 years of operating conditions demonstrate that FBMC and ATCMC

attain very similar performance. The major policy message of the paper is to challenge whether it is worth for more European countries to switch from ATCMC to FBMC, instead of advancing directly to a nodal design.

The paper is organized as follows. Section 2 introduces our modeling framework for transmission capacity allocation in zonal markets using linear programs that capture the most important differences in the alternative market designs. These simplified models permit an analysis of the differences with respect to the nodal design and the FBMC methodology implemented in the CWE. Section 3 develops cutting-plane algorithms for simulating the nodal design, FBMC and ATCMC under the N-1 security criterion. Section 4 presents the large-scale CWE system used in the realistic case study, and section 5 presents the main numerical results and discusses the implications of these results for zonal electricity markets. Finally, section 6 concludes the paper and outlines directions for future research.

2. Transmission capacity allocation in electricity markets

Transmission capacity allocation mechanisms include (i) forward contracts, for instance, the long-term auctions carried out by the Joint Allocation Office (2015), and (ii) different types of implicit allocation, typically used in day-ahead electricity markets (Schweppe et al. 1988). In the following, we focus on day-ahead electricity markets and describe each policy for transmission capacity allocation (nodal, FBMC and ATCMC) in its simplest form in order to better understand the differences between them. We adopt the following assumptions: (i) demand is fixed and only producers bid in the market, (ii) all market participants act as price-takers (i.e. they bid their true cost to the market), and (iii) all energy is traded in the day-ahead auction (i.e. we ignore long-term contracts and bilateral trades). The latter implies that we also ignore the intraday market. This assumption is adopted in order to simplify the analysis. However, we note that the intraday markets are also organized as zonal markets, and therefore are exposed to the same inefficiencies stemming from the inaccurate representation of the transmission network as zonal day-ahead markets.

2.1. Nodal electricity markets

Nodal electricity markets use Locational Marginal Pricing (LMP), first proposed by Schweppe et al. (1988), in order to price electricity at every node of the system, while accounting for transmission congestion in a DC approximation of the real network equations. Under our assumptions, the LMP day-ahead market can be cleared by solving the optimization problem (1) – (3):

$$\min_{v\in[0,1],f,\theta} \quad \sum_{g\in G} P_g Q_g v_g \tag{1}$$

$$\text{s.t.} \quad \sum_{g\in G(n)} Q_g v_g - \sum_{l\in L(n,\cdot)} f_l + \sum_{l\in L(\cdot,n)} f_l = Q_n \quad \forall n\in N \quad [\rho_n] \tag{2}$$

$$-F_l \le f_l \le F_l,\ f_l = B_l\left(\theta_{m(l)} - \theta_{n(l)}\right) \quad \forall l\in L. \tag{3}$$

The notation in this model is as follows: Q_g, P_g correspond to the quantity and price bid by generator $g\in G$; $G(n)$ is the set of generators at node n; Q_n is the forecast demand at node $n\in N$; $F_l, B_l, m(l), n(l)$ are the thermal limit, susceptance, and adjacent nodes (in the outgoing and incoming direction respectively) of line $l\in L$; $L(m,n)$ is the set of lines directed from node m to node n; v_g is the acceptance/rejection decision for the bid placed by generator g; f_l is the flow through line l; and θ_n is the voltage angle at node n.

The objective function (1) corresponds to the total operation cost, constraints (2) enforce nodal power balance, and constraints (3) model the DC transmission constraints. Prices ρ_n can be obtained as the dual multipliers of constraints (2).

Note that we use the acceptance level v_g as a decision variable, following academic literature related to European electricity markets (Van den Bergh et al. 2016, Aravena and Papavasiliou 2017). This differs from the formulation which represents the output of generators as decision variables, and is more common in the literature related to nodal markets. This differs from the formulation which represents the output of generators as decision variables, and is more common in the literature related to nodal markets. The formulation that we employ here offers the advantage that its linear programming dual has as variable the surplus of each bid/generator, unscaled, which

is useful when enforcing pricing restrictions for discrete bids (see section EC.3 of the electronic companion). In addition, we use the B-theta formulation instead of the one based on Power Transfer Distribution Factors (PTDF). The B-theta formulation is more convenient for representing line contingencies, as we discuss in section 3.1.

The LMP policy implicitly allocates the capacity of all lines in the system, without any distinction between zones, and while respecting the network constraints. This implies that, absent any uncertainty (such as renewable energy forecast errors or outages), the optimal acceptance/rejection decisions v^* can be implemented directly in the system without violating any technical constraint.

2.2. Zonal electricity markets

In zonal electricity markets, electricity is priced at a zonal level, and nodal level information is discarded (Ehrenmann and Smeers 2005). Bids are associated to zones instead of nodes, and transmission constraints can only be imposed at a zonal level. A zonal market can be cleared by solving problem (4) – (6):

$$\min_{v\in[0,1],p} \sum_{g\in G} P_g Q_g v_g \tag{4}$$

$$\text{s.t.} \quad \sum_{g\in G(z)} Q_g v_g - p_z = \sum_{n\in N(z)} Q_n \quad \forall z \in Z \quad [\rho_z] \tag{5}$$

$$p \in \mathcal{P}, \tag{6}$$

where p_z corresponds to the net position of zone $z \in Z$, $G(z), N(z)$ correspond to the set of generators and nodes in zone z, and $\mathcal{P}$ corresponds to the feasible set of net positions. $\mathcal{P}$ is a convex polyhedron which is defined differently for each inter-zonal capacity allocation mechanism, but always respects power balance, i.e. $\sum_z p_z = 0$. In this model, constraints (5) define the zonal net positions, and constraint (6) enforces that the zonal net positions belong in $\mathcal{P}$.

European regulations set forth guidelines for defining $\mathcal{P}$. Annex I of Regulation (EC) 2009/714 establishes that "... *TSOs shall endeavour to accept all commercial transactions, including those involving cross-border-trade* ..." (Article 1.1) and that "... *TSOs shall not limit interconnection*

capacity in order to solve congestion inside their own control area, save for the abovementioned reasons and reasons of operational security ..." (Article 1.7). At the same time, Regulation (EU) 2015/1222 requires allocated cross-border capacity to be firm (Article 69)[2]. In the spirit of these regulations, $\mathcal{P}$ should include all net position configurations p that are feasible with respect to the real grid and exclude those that can be proven to lead to unsafe operating conditions. We describe three methodologies for defining $\mathcal{P}$: FB with GSKs, FB with exact projection, and ATC with exact projection.

2.2.1. Flow-based methodology with Generation Shift Keys. This methodology is currently used in the implementation of FBMC in the CWE (50Hertz et al. 2017). The first step in the method is to determine GSKs for each generator within each zone. GSKs quantify the change in the output of generators that would result from a change in zonal net positions with respect to a base case dispatch, i.e. $GSK_g = Q_g \Delta v_g / \Delta p_{z(g)}$. GSKs, along with the node-to-line PTDF matrix, are used to compute zone-to-line PTDFs as $PTDF_{l,z} = \sum_{g \in G(z)} GSK_g \cdot PTDF_{l,n(g)},\ \forall l \in L, z \in Z$. Here, $n(g)$ corresponds to the node at which generator g is located, and $PTDF_{l,n}$ is the Power Transfer Distribution Factor of line l and node n. Zone-to-line PTDFs are the equivalent of node-to-line PTDFs when the nodes are aggregated into zones. Their computation, however, is more challenging: one needs to assume how an additional injection of 1MW in a zone decomposes into nodal injections in that zone (which is exactly the role of GSKs). Then, using the base case dispatch (denoted with a zero superscript), the flow across each line is approximated as $f_l \approx f_l^0 + \sum_{z \in Z} PTDF_{l,z} \cdot (p_z - p_z^0),\ \forall l \in L$.

If, for a certain line $l \in L$ and any zone $z \in Z$, $PTDF_{l,z}$ is larger than 5%, then l is considered to be a Critical Branch (CB). For each Critical Branch, TSOs determine its corresponding Remaining Available Margin (RAM) starting from the thermal capacity of the branch minus the flow on the base case ($F_l - f_l^0$), subtracting the Flow Reliability Margin, and adding the Final Adjustment Value. Finally, the set of feasible net positions with GSKs, $\mathcal{P}^{FB-GSK}$, is described by

$$\mathcal{P}^{FB-GSK} = \left\{ p \in \mathbb{R}^{|Z|} \;\middle|\; \sum_{z \in Z} p_z = 0,\ \sum_{z \in Z} PTDF_{cb,z} \cdot p_z \leq RAM_{cb}\ \forall cb \in CB \right\}. \tag{7}$$

We denote by FBMC-GSK the flow-based market clearing problem (4) – (6) with $\mathcal{P} = \mathcal{P}^{FB-GSK}$.

The methodology has several points where discretionary decisions are made by TSOs. These include the selection of a base case, the determination of GSKs, the selection of Critical Branches, and the determination of Flow Reliability Margins and Final Adjustment Values, all of which are subject to the discretion of the TSOs. Indeed, different TSOs use different criteria for certain choices (50Hertz et al. 2017, CREG 2017). Additionally, $\mathcal{P}^{FB-GSK}$ will only be a good representation of reality whenever the flows on critical branches are approximated accurately. Unfortunately, this cannot be guaranteed (Waniek et al. 2010). Furthermore, a circularity problem arises: the better TSOs can anticipate the outcome of the market, the closer the base case would be to reality and, consequently, power flows would be approximated more accurately. However, the outcome of the market depends on the parameters decided by TSOs. In addition, the definition of these parameters grants a certain degree of flexibility to the TSOs. This can lead to situations where TSOs anticipate the generation costs of the units in their control area and prevent certain net positions that correspond to unlikely generating patterns from being cleared. Not only are these practices very difficult to model, but they also contravene the principle of non-discrimination which underlies European legislation. These problems, among others, have placed the FBMC-GSK methodology under scrutiny by National Regulatory Authorities, see EI and NVE (2017) and CREG (2017).

2.2.2. Flow-based methodology with exact projection. Instead of resorting to assumptions for approximating power flows using zonal net positions, we can determine the exact set of feasible net positions $\mathcal{P}^{FB-EP}$ with respect to the actual grid by projecting the power flow equations onto the space of net positions:

$$\begin{aligned}\mathcal{P}^{FB-EP} = \Bigg\{ p \in \mathbb{R}^{|Z|} \;\Bigg|\; & \exists (\bar{v}, f, \theta) \in [0,1]^{|G|} \times \mathbb{R}^{|L|} \times \mathbb{R}^{|N|} : \\ & \sum_{g \in G(z)} Q_g \bar{v}_g - p_z = \sum_{n \in N(z)} Q_n \quad \forall z \in Z, \\ & \sum_{g \in G(n)} Q_g \bar{v}_g - \sum_{l \in L(n,\cdot)} f_l + \sum_{l \in L(\cdot,n)} f_l = Q_n \quad \forall n \in N, \\ & -F_l \le f_l \le F_l, \; f_l = B_l \left(\theta_{m(l)} - \theta_{n(l)} \right) \quad \forall l \in L \Bigg\}.\end{aligned} \tag{8}$$

This set includes all zonal net positions for which there exists at least one vector of generator output levels that is feasible under the full network model. The set $\mathcal{P}^{FB-EP}$ is not currently used in EU market operations. It is rather a mathematical definition of the flow-based domain that allows for an objective quantitative comparison of a very broad family of aggregation models (including FBMC and ATCMC). Indeed, as it will be shown in the next section, this definition can easily be extended to compute ATCs. Using $\mathcal{P}^{FB-EP}$ in (6) has four main advantages over other alternatives: (i) it is a natural way to approach an aggregation model, as it corresponds to the projection of the set of feasible nodal injections to the space of zonal net positions, (ii) it does not require any assumptions or discretionary parameters, (iii) it allows all trades that are feasible with respect to the real network to be cleared, and (iv) it prevents all trades that can be proven to be impossible from being cleared. Note that implementing this approach requires information about the grid, the installed generation capacity and the forecast demand at each node, all of which are already available to system operators. No information about the price or attribution of the bids to nodes is necessary.

One fundamental characteristic of our proposal to use the set $\mathcal{P}^{FB-EP}$ for zonal market clearing is that it fully separates the representation of the grid (i.e. the polytope $\mathcal{P}^{FB-EP}$) from dispatch considerations. This is in contrast with the existing method that relies on GSKs, according to which the representation of the grid depends on the dispatch. It is the inclusion of the dispatch considerations in the representation of the grid that leads to a limitation of cross-border exchanges that is known to exist with the current methodology, see ACER (2018).

We note that, under the assumption that market participants bid truthfully, the quantity bid by generator g is equal to its capacity. This is why parameter Q_g appears both in the market clearing problem (4) – (6) and in the definition of the polytope in equation (8).

2.2.3. Available-transfer-capacity methodology with exact projection. The ATC methodology defines a set of interconnectors T between neighboring zones, each $t \in T$ comprising cross-border lines $L(t) \subseteq L$, and assigns a maximum capacity in the forward (ATC_t^+) and backward

(ATC_t^-) direction for each interconnector. These capacities are determined in a series of steps, analogous to those presented in subsection 2.2.1, aiming at computing simultaneous limits on cross-border exchanges between pairs of neighboring zones, see APX Group et al. (2010) and Aravena and Papavasiliou (2017). We abstract from these discretionary considerations and, following the principle that $\mathcal{P}$ should include the largest possible subset of feasible net position configurations, Regulation (EC) 2009/714, we compute ATCs by solving the optimization problem (9) – (11):

$$\max_{ATC} \prod_{t\in T} \left(ATC_t^- + ATC_t^+\right) \tag{9}$$

$$\text{s.t.} \quad -ATC_t^- \leq ATC_t^+ \quad \forall t \in T \tag{10}$$

$$[-ATC^-, ATC^+] \subseteq \mathcal{E}^{EP}, \tag{11}$$

where $[-ATC^-, ATC^+] \subseteq \mathbb{R}^{|T|}$ is the rectangle with lower vertex $-ATC^-$ and upper vertex ATC^+, and $\mathcal{E}^{EP}$, defined in (12), is the feasible domain of cross-border exchanges:

$$\begin{aligned}\mathcal{E}^{EP} = \Bigg\{ e \in \mathbb{R}^{|T|} \Bigg| & -\sum_{l\in L(t)} F_l \leq e_t \leq \sum_{l\in L(t)} F_l \quad \forall t \in T, \\ & \exists p \in \mathcal{P}^{FB-EP} : p_z = \sum_{t\in T(z,\cdot)} e_t - \sum_{t\in T(\cdot,z)} e_t \quad \forall z \in Z \Bigg\}.\end{aligned} \tag{12}$$

Problem (9) – (11) seeks to maximize the volume of the rectangle formed by the ATC values of all interconnectors, while ensuring that (i) the cross-border exchange between each pair of zones is bounded by their total interconnection capacity, and (ii) the net positions at each exchange configuration within the ATC rectangle are feasible with respect to the real network constraints (TenneT 2014).

Once the ATC values are available from solving problem (9) – (11), the feasible net position domain under the ATC methodology with exact projection, $\mathcal{P}^{ATC-EP}$, can be defined as:

$$\begin{aligned}\mathcal{P}^{ATC-EP} = \Bigg\{ p \in \mathbb{R}^{|Z|} \Bigg| \; \exists e \in \mathbb{R}^{|T|} : \; & p_z = \sum_{t\in T(z,\cdot)} e_t - \sum_{t\in T(\cdot,z)} e_t \quad \forall z \in Z, \\ & -ATC_t^- \leq e_t \leq ATC_t^+ \quad \forall t \in T \Bigg\}.\end{aligned} \tag{13}$$

In contrast with $\mathcal{P}^{FB-GSK}$, defined in (7), and $\mathcal{P}^{FB-EP}$, defined in (8), where we enforce zonal balance explicitly, $\mathcal{P}^{ATC-EP}$ enforces zonal power balance implicitly, because the interconnectors

define a transportation network between the zones. We use the same naming convention than for the flow-based methodology with GSKs: we denote by FBMC-EP (resp. ATCMC-EP) the flow-based market clearing problem (4) – (6) with $\mathcal{P} = \mathcal{P}^{FB-EP}$ (resp. $\mathcal{P} = \mathcal{P}^{ATC-EP}$).

2.3. Feasible domain comparison

The feasible set of zonal net positions differs among policies. Denote by $\mathcal{P}^{LMP}$ the feasible set of zonal net positions of the LMP policy. Then, by construction, we have that $\mathcal{P}^{LMP} = \mathcal{P}^{FB-EP} \supseteq \mathcal{P}^{ATC-EP}$, while $\mathcal{P}^{FB-GSK}$ is not comparable to the previous sets. Thus, while FBMC-EP allows all possible inter-zonal exchange schedules, ATCMC-EP might not allow some of them, but FBMC-EP and ATCMC-EP will not allow clearing with an infeasible cross-border exchange schedule. FBMC-GSK, on the other hand, might prevent feasible net positions from being cleared and allow infeasible net positions to be cleared, as we demonstrate with a simple numerical example in section 2.4. This implies that the current practice for FBMC, FBMC-GSK, is in direct violation of Regulation (EC) 2009/714, whereas the models that we propose, FBMC-EP and ATCMC-EP, obey European regulations.

The feasible set of acceptance/rejection of bids is another interesting point of comparison. Let us define the feasible set of acceptance/rejection of bids of each policy as:

$$\begin{aligned}
\mathcal{V}^{LMP} &= \{v \in [0,1]^{|G|} \mid \exists (f,\theta),(v,\theta,f) \text{ respecting (2) – (3)}\},\\
\mathcal{V}^{FB-GSK} &= \{v \in [0,1]^{|G|} \mid \exists p,(v,p) \text{ respecting (5) – (6) with } \mathcal{P} := \mathcal{P}^{FB-GSK}\},\\
\mathcal{V}^{FB-EP} &= \{v \in [0,1]^{|G|} \mid \exists p,(v,p) \text{ respecting (5) – (6) with } \mathcal{P} := \mathcal{P}^{FB-EP}\} \text{ and}\\
\mathcal{V}^{ATC-EP} &= \{v \in [0,1]^{|G|} \mid \exists p,(v,p) \text{ respecting (5) – (6) with } \mathcal{P} := \mathcal{P}^{ATC-EP}\}.
\end{aligned}$$

Then, we have that $\mathcal{V}^{LMP} \subseteq \mathcal{V}^{FB-EP} \supseteq \mathcal{V}^{ATC-EP}$, while $\mathcal{V}^{FB-GSK}$ is not comparable with the previous sets. This implies that, although FBMC-EP and ATCMC-EP are guaranteed to clear with a feasible cross-border exchange schedule $p_z, z \in Z$, the acceptance/rejection decisions for bids obtained by these models might not be feasible for the real network.

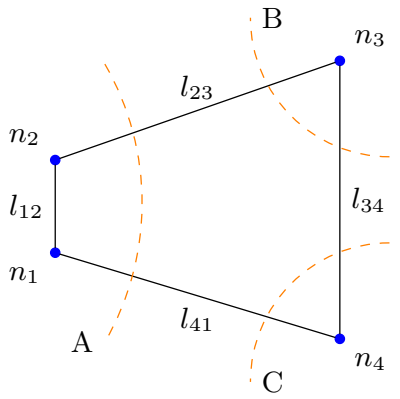

Generators

g	$n(g)$	Q_g [MW]	P_g [$/MWh]
1	n_1	500	8
2	n_2	200	45
3	n_3	300	18
4	n_4	500	200

Consumers

n	Q_n [MW]
n_2	300
n_4	300

Figure 1 4-node, 3-zone network data of section 2.4. All lines have equal impedance.

2.4. Policy comparison using an illustrative example

We compare LMP, FBMC-GSK, FBMC-EP and ATCMC-EP using the 4-node, 3-zone network presented in Fig. 1. We investigate cases of inter- and intra-zonal scarce transmission capacity. In both cases, we solve the LMP model (1) – (3) directly and the FBMC-GSK model (4) – (6), with $\mathcal{P} \equiv \mathcal{P}^{FB-GSK}$, using the GSK strategy of the Belgian TSO (50Hertz et al. 2017). We solve the FBMC-EP model (4) – (6), with $\mathcal{P} \equiv \mathcal{P}^{FB-EP}$, by explicitly describing $\mathcal{P}^{FB-EP}$ in the lifted space of $\bar{v}, f, \theta$ using its definition (8). Concretely, this means that the market clearing problem is solved as one single optimization model that includes extended variables $\bar{v}, f, \theta$. Similarly, we solve the ATC computation model (9) – (11) by explicitly modeling all vertices $\nu \in \mathcal{V}$ of the rectangle $[-ATC^-, ATC^+]$, and enforcing that the corresponding exchange limit e^ν of each vertex $\nu \in \mathcal{V}$ is a feasible cross-border exchange configuration, i.e. $e^\nu \in \mathcal{E}^{EP}$. Here $\mathcal{E}^{EP}$ is described on the lifted space of variables $p^\nu, \bar{v}^\nu, f^\nu, \theta^\nu$ using its definition (12). The computed ATC values are then used to solve the ATCMC-EP model (4) – (6), with $\mathcal{P} \equiv \mathcal{P}^{ATC-EP}$, which is solved directly. The goal of this example is to illustrate the abstract FBMC-EP concept in a concrete setting.

2.4.1. Inter-zonal scarce transmission capacity. In order to study the behavior of the different policies under inter-zonal scarce transmission capacity, we clear the market for the system of Fig. 1 with the thermal capacity of line l_{41} assumed equal to 100 MW. All other lines are assumed to have unlimited capacity.

Policy	Total cost [$]	Abs. error flow approx. [MW]	Overload l_{41} [MW]
LMP	15 200	0	0
FBMC-GSK	7 217	475	79
FBMC-EP	7 800	300	50
ATCMC-EP	23 208	–	50

Table 1 Summary of clearing quantities for a case of inter-zonal congestion (l_{41} limited to 100 MW). Flow approximation absolute error refers to the sum over all lines of the difference between model flows (i.e. flows inside the definitions of $\mathcal{P}^{FB-GSK}$ in (7) and of $\mathcal{P}^{FB-EP}$ in (8)) and implied flows (i.e. flows that would transit over the lines in the network if the optimal decisions of each policy v^* were implemented).

Table 1 presents a summary of the clearing results. We find that all zonal policies clear with acceptance/rejection decisions that result in infeasible flows for the real network (5^{th} column), and that FBMC-GSK leads to a larger approximation error (4^{th} column) than FBMC-EP. We present the feasible domains of net positions for each model in Fig. 2. It is interesting to observe that LMP and FBMC-EP clear with the same net positions. Nevertheless, the LMP acceptance/rejection decisions are feasible for the real network, while the decisions of FBMC-EP are not. This occurs because of the difference in price and location of bids within zone A. Zonal policies will accept these bids following the merit order, in the sense of accepting the bid at n_1 fully before accepting any part of the bid at n_2. This decision, however, leads to overloading line l_{41}. According to FBMC-EP, this decision is feasible because there exist at least one $\bar{v}$ with the same net positions (for instance, the optimal decision of the LMP policy).

FBMC-GSK clears with a cross-border exchange schedule that is infeasible for the real network. Note also that the set $\mathcal{P}^{FB-GSK}$ does not include a slice of $\mathcal{P}^{FB-EP}$ (containing feasible net positions for the real network) shaded with horizonal gray lines in Fig. 2. In other words, FBMC-GSK fails to accurately account for cross-border exchanges, and distorts the market outcome due to discretionary parameters used for approximating power flows on lines.

2.4.2. Intra-zonal scarce transmission capacity. In order to study the effect of intra-zonal congestion, we use the same system of Fig. 1, where we now constrain the thermal capacity of line

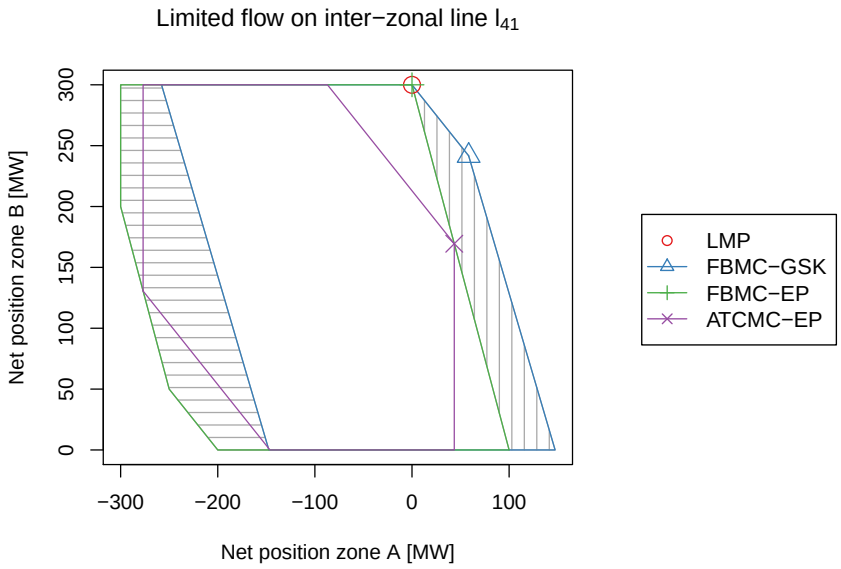

Figure 2 Set of feasible net positions on plane A-B for a case of inter-zonal congestion (l_{41} limited to 100 MW). The net position of zone C is implied by the net positions of A and B because of energy balance. The points indicate the zonal net positions at the optimal solution for each policy. The area shaded with horizonal gray lines corresponds to $\mathcal{P}^{FB-EP} - \mathcal{P}^{FB-GSK}$ (feasible net positions prohibited in FBMC-GSK) and the area shaded with vertical gray lines corresponds to $\mathcal{P}^{FB-GSK} - \mathcal{P}^{FB-EP}$ (infeasible net positions allowed in FBMC-GSK).

l_{12} to 100 MW and assume an unlimited capacity for all other lines. We employ the same GSKs as in the previous subsection.

We can observe in table 2 that all zonal policies clear with acceptance/rejection decisions that are infeasible for the real network. As in the case of inter-zonal congestion, the flows estimated by FBMC-GSK are a less accurate approximation than those estimated by FBMC-EP. Interestingly, the estimated flows in FBMC-GSK can be in the opposite direction of the flows implied by the DC power flow equations. As shown in Fig. 3, for this case $\mathcal{P}^{FB-GSK}$ turns out to be a relaxation of $\mathcal{P}^{FB-EP}$.

In summary, zonal markets fail to properly allocate scarce transmission capacity both when inter-zonal and intra-zonal congestion arises. FBMC-EP outperforms FBMC-GSK in accuracy while not introducing market distortions. For this reason, in what follows, we will only consider FBMC-EP and will refer to it simply as FBMC. Similarly, we refer to ATCMC-EP simply as ATCMC.

Policy	Total cost [$]	Abs. error flow approx. [MW]	Overload l_{12} [MW]
LMP	10 267	0	0
FBMC-GSK	5 800	536	150
FBMC-EP	5 800	300	150
ATCMC-EP	9 750	–	108

Table 2 Summary of clearing quantities for a case of intra-zonal congestion (l_{12} limited to 100 MW).

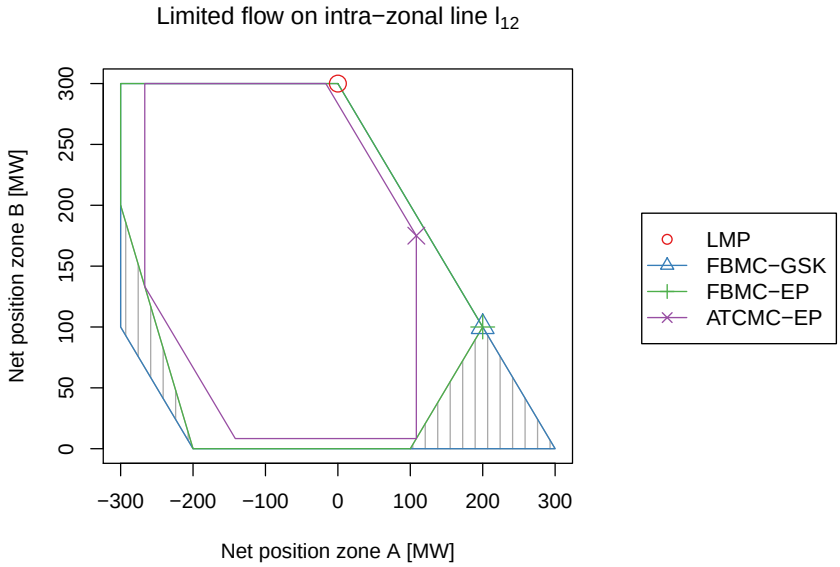

Figure 3 Feasible net position set on plane A-B for a case of intra-zonal congestion (l_{12} limited to 100MW). The points indicate the zonal net positions at the optimal solution for each policy. The area shaded with vertical gray lines corresponds to $\mathcal{P}^{FB-GSK} - \mathcal{P}^{FB-EP}$.

3. Cutting-plane algorithms for market clearing under the N-1 security criterion

Electricity market operations ensure reliability by protecting the system against two types of uncertainty: (i) unpredictable changes in supply or demand, and (ii) contingencies related to unplanned outages of certain system elements. A commonly employed rule of thumb for ensuring reliable system operation is the N-1 security criterion (Regulation (EU) 2017/1485), (CAISO 2015, Grid Optimization Competition 2018), whereby network operators set reserve targets in order to protect the system against generating unit outages and branch outages. The N-1 security criterion interacts with European day-ahead market clearing, and it is necessary to account for this interaction

in order to produce results with policy relevance in a case study[3]. This is the main motivation for extending our models to N-1 robustness in the present section. A secondary motivation of this section is to demonstrate that our modeling framework is sufficiently flexible to include particular idiosyncrasies of zonal markets. Another example of a feature that can be easily accounted for within our modeling framework is strict linear pricing (which is the European approach for dealing with the pricing of non-divisibilities), to which our models are extended in section EC.3 of the electronic companion.

Modeling generation contingencies in the case of LMP is more complicated. One way to model generation contingencies in a nodal setting is to use so-called "participation factors" (Grid Optimization Competition 2018). Participation factors are used for representing primary reserves (droop control and automatic generation control, AGC, i.e. primary and secondary reserve in EU nomenclature), whereas operating reserves (which correspond to tertiary reserve in EU nomenclature) are represented in both the zonal and nodal models through reserve requirements. We therefore avoid double-counting this level of security in the system by only including transmission line contingencies in the nodal and zonal day-ahead market clearing models. Notwithstanding, our real-time simulations also account for generator failures.

The algorithms that we develop in this section have been inspired by the algorithm proposed by Street et al. (2014) for security-constrained unit commitment. In this work, the authors use a cutting-plane procedure in order to progressively improve an under-approximation of the worst-case curtailment of demand after a contingency as a function of the commitment decisions, while considering dispatch decisions as a recourse. In contrast, our algorithms generate (i) descriptions of the feasible set of injections for LMP, considering dispatch decisions as first-stage variables, and (ii) descriptions of the inclusion constraints (6) and (11). We base these descriptions on distance functions that become zero if and only if the corresponding inclusion constraints are respected. In what follows, subsection 3.1 presents our cutting-plane algorithm for solving (1) – (3) and subsection 3.2 presents a similar technique for solving (4) – (6), under the N-1 security criterion.

Proofs for the propositions presented in this section and an algorithm for solving (9) – (11), which uses the same ideas as the algorithm of section 3.2, are presented in section EC.1 of the electronic companion.

3.1. Decomposition algorithm for nodal electricity markets with N-1 security

Following current industry standards (Grid Optimization Competition 2018), we define N-1 security for LMP markets as the ability of a system to withstand any single-element transmission contingency, while maintaining its current nodal injections and without violating any operating limits. The nodal injection r_n at node n corresponds to $\sum_{g\in G(n)} Q_g v_g - Q_n$ and the security constraints correspond to generation and transmission limits. A nodal electricity market under the N-1 security criterion can then be cleared by solving

$$\min_{v\in[0,1],r} \quad \sum_{g\in G} P_g Q_g v_g \tag{14}$$

$$\text{s.t.} \quad \sum_{g\in G(n)} Q_g v_g - r_n = Q_n \quad \forall n\in N \quad [\rho_n] \tag{15}$$

$$r \in \mathcal{R}_{N-1} \tag{16}$$

where $\mathcal{R}_{N-1}$ is the feasible set of injections under any single-element transmission contingency, i.e. $\mathcal{R}_{N-1} = \cap_{\substack{u\in\{0,1\}^{|L|}\\ \|u\|_1\le 1}} \mathcal{R}(u)$ with

$$\mathcal{R}(u) = \left\{ \bar{r}\in\mathbb{R}^n \;\middle|\; \exists (f,\theta)\in\mathbb{R}^{|L|}\times\mathbb{R}^{|N|}: \sum_{l\in L(n,\cdot)} f_l - \sum_{l\in L(\cdot,n)} f_l = \bar{r}_n \quad \forall n\in N, \right.$$
$$\left. -F_l \le f_l \le F_l,\ f_l = B_l(1-u_l)\left(\theta_{m(l)} - \theta_{n(l)}\right) \quad \forall l\in L \right\}. \tag{17}$$

The main idea behind our decomposition algorithm for LMP under N-1 security is to replace the inclusion constraint (16) by a polyhedral outer approximation which is tight at the optimal solution (v^*, r^*). This polyhedral outer approximation can be expressed as $\{r\in\mathbb{R}^n \mid \sum_{n\in N} V_{m,n} r_n \le W_m \quad \forall m = 1,\dots,M\} \supseteq \mathcal{R}_{N-1}$, where M is the number of hyperplanes of the approximation. Following this reasoning, we propose clearing the market under LMP using Alg. 1, which is based on repeatedly calling two oracles:

Algorithm 1 Cutting-plane algorithm for solving LMP under N-1 security.

1: Initialize $V := 0_{1,|N|}, W := 0$, `inclusion` := `FALSE`
2: **while** !`inclusion` **do**
3: Call $NMCO(V, W) \to r$
4: Call $IO(r) \to$ `inclusion`, (v, w)
5: $V := [V^\top \ v]^\top, \ W := [W^\top \ w]^\top$
6: **end while**
7: Terminate: inner model of $NMCO(V, W)$ gives the optimal clearing.

- A nodal market-clearing oracle $NMCO(V, W)$ which, for a given $V \in \mathbb{R}^{M \times |N|}$ and $W \in \mathbb{R}^M$, solves the relaxed LMP clearing problem $\{(14), (15), Vr \leq W\}$ and returns a vector of optimal nodal injections r^*.
- An injection oracle $IO(r)$ which, for a given vector of nodal injections r, either certifies that $r \in \mathcal{R}_{N-1}$, or returns a hyperplane that separates r from $\mathcal{R}_{N-1}$.

While the market clearing oracle operations are clearly defined (they consist of solving a linear program), there are several ways in which we could devise an injection oracle, and the effectiveness of Alg. 1 in handling realistic instances will depend on the specific injection oracle that we employ. For example, an oracle that produces a deep separating hyperplane but relies on checking all N-1 contingencies one-by-one would not be effective in practice. With this in mind, we design our injection oracle based on the observation that (16) can be described equivalently in terms of a point-to-set distance function, i.e. $r \in \mathcal{R}_{N-1}$ if and only if $d(r, R_{N-1}) = 0$ for any distance function d. Concretely, given the definition of $\mathcal{R}_{N-1}$ we consider the following distance function:

$$d(r, \mathcal{R}_{N-1}) = \max_{\substack{u \in \{0,1\}^{|L|} \\ \|u\|_1 \leq 1}} \ \min_{\bar{r} \in \mathcal{R}(u)} \ \|r - \bar{r}\|_1,$$

which is defined using a bi-level mathematical program. The inner problem can be cast as a linear program which we can dualize and derive an alternative definition of $d(\bar{r}, \mathcal{R}_{N-1})$ as a bi-linear

program:

$$\begin{aligned} d(r,\mathcal{R}_{N-1}) \;= \max_{u,\gamma,\phi,\rho} \quad & -\sum_{n\in N} r_n\rho_n - \sum_{l\in L} F_l(\gamma_l^- + \gamma_l^+) \\ \text{s.t.} \quad & -1 \le \rho_n \le 1 \quad \forall n \in N \\ & -\gamma_l^- + \gamma_l^+ + \phi_l - \rho_{n(l)} + \rho_{m(l)} = 0 \quad \forall l \in L \\ & \sum_{l\in L(n,\cdot)} B_l(1-u_l)\phi_l + \sum_{l\in L(\cdot,n)} B_l(1-u_l)\phi_l = 0 \quad \forall n \in N \\ & \gamma \ge 0,\, u \in \{0,1\}^{|L|},\, \|u\|_1 \le 1. \end{aligned} \tag{18}$$

We then employ an injection oracle based on distance (IOD) in the implementation of Alg. 1, which performs the following operations for every query point r:

1. Compute $\tilde{w} := d(r,\mathcal{R}_{N-1})$ and obtain a subgradient $v \in \partial_r d(r,\mathcal{R}_{N-1})$ (v corresponds to $-\rho^*$).
2. If $\tilde{w} = 0$, then return `TRUE`, $(0_{|N|}, 0)$.
3. Else return `FALSE`, $(v, -\tilde{w} + v^T r)$.

Using IOD we can prove the following:

PROPOSITION 1. *Algorithm 1 terminates with an optimal solution in a finite number of iterations when using IOD as injection oracle.*

Note that we do not need to solve (18) as a bi-linear program when computing $d(r,\mathcal{R}_{N-1})$. Instead, we can use a mixed integer linear reformulation where the products between variables are relaxed using their McCormick envelopes (McCormick 1976). Since u is binary, this is an exact relaxation. IOD, then, avoids exhaustively checking all N-1 contingencies and it only checks those that show promise within a branch-and-bound scheme. We further speedup IOD by allowing it to return sub-optimal solutions to (18) as long as their value exceeds a positive cutoff, thereby also providing an infeasibility certificate and a valid separating hyperplane. Incorporating these improvements, IOD achieves practical performance on instances of realistic scale, such as those considered in the case study of section 4.

3.2. Decomposition algorithm for flow-based market coupling with N-1 security

The notion of N-1 security in zonal markets requires that systems be able to withstand any single-element transmission contingency, while maintaining zonal net positions, without violating any security constraints (RTE 2006, 50Hertz et al. 2017). Note that this notion allows for remedial actions that preserve net positions following a transmission contingency, which is in contrast with the current practice in nodal markets, where no remedial actions are considered.

The FBMC problem under N-1 security can then be posed as $\{(4),\ (5),\ p \in \mathcal{P}^{FB-EP}_{N-1} = \cap_{\substack{u\in\{0,1\}^{|L|} \\ \|u\|_1\leq 1}} \mathcal{P}^{FB-EP}(u)\}$, where $\mathcal{P}^{FB-EP}_{N-1}$ is the feasible net position domain under any single-element transmission contingency and $\mathcal{P}^{FB-EP}(u)$ corresponds to

$$\begin{aligned}\mathcal{P}^{FB-EP}(u) = \Bigg\{ p \in \mathbb{R}^{|Z|} \Bigg| \exists (\bar{v}, f, \theta) \in [0,1]^{|G|} \times \mathbb{R}^{|N|} \times \mathbb{R}^{|L|} : \\ \sum_{g\in G(z)} Q_g \bar{v}_g - p_z = \sum_{n\in N(z)} Q_n \ \forall z \in Z, \\ \sum_{g\in G(n)} Q_g \bar{v}_g - \sum_{l\in L(n,\cdot)} f_l + \sum_{l\in L(\cdot,n)} f_l = Q_n \ \forall n \in N, \\ -F_l \leq f_l \leq F_l,\ f_l = B_l(1-u_l)\left(\theta_{m(l)} - \theta_{n(l)}\right)\ \forall l \in L \Bigg\}.\end{aligned}$$

This formulation of the FBMC clearing problem under N-1 security ensures that the market clears with a net position that (i) is feasible under the no-contingency case and (ii) that can be maintained through remedial actions under any single-element transmission contingency. This definition of the flow-based domain also implies that the feasible sets of net positions may differ between zonal and nodal markets under N-1 security, a result that we formalize in Prop. 2. In words, this proposition implies that the nodal N-1 security criterion imposes more conservative limits on inter-zonal exchanges than its zonal counterpart, according to the current regulation of European markets.

PROPOSITION 2. *Let $\mathcal{P}^{LMP}_{N-1}$ be the feasible set of zonal net positions of the nodal market under N-1 security, i.e. the projection of $\{(v,r) \in [0,1]^{|G|} \times \mathbb{R}^{|N|} \mid (15), (16)\}$ onto the zonal net position space. Then $\mathcal{P}^{LMP}_{N-1} \subseteq \mathcal{P}^{FB-EP}_{N-1}$.*

We solve the FBMC clearing problem under N-1 security using an analogous strategy to the one used for nodal markets in the previous section. Concreteley, we replace the inclusion constraint $p \in \mathcal{P}_{N-1}^{FB-EP}$ by a polyhedral outer approximation, $\sum_{z\in Z} V_{m,z} p_z \leq W_m \quad \forall m = 1,\ldots,M$, which is tight at the optimal solution p^*. The outer approximation is progressively constructed by querying the distance function

$$d(p, \mathcal{P}_{N-1}^{FB-EP}) = \max_{\substack{u\in\{0,1\}^{|L|} \\ \|u\|_1 \leq 1}} \; \min_{\bar{p}\in\mathcal{P}^{FB-EP}(u)} \; \|p - \bar{p}\|_1, \tag{19}$$

which becomes zero if and only if $p \in \mathcal{P}_{N-1}^{FB-EP}$. The evaluation of this distance function requires solving a mixed-integer linear program, from the solution of which we can generate a separating hyperplane whenever $p \notin \mathcal{P}_{N-1}^{FB-EP}$. Then, we follow the procedure described in Alg. 1 for solving the FBMC clearing problem under N-1 security, replacing $NMCO$ and IO, respectively, with:

- a zonal market-clearing oracle $ZMCO(V,W)$ which, for a given $V \in \mathbb{R}^{M\times|Z|}$ and $W \in \mathbb{R}^M$, solves the FBMC clearing problem using $Vp \leq W$ as a substitute for $p \in \mathcal{P}_{N-1}^{FB-EP}$, and returns a vector of optimal net positions p^*, and
- a net position oracle based on distance $NPOD(p)$ which, for a given vector of net positions p evaluates $d(p, \mathcal{P}_{N-1}^{FB-EP})$ and, either, certifies that $p \in \mathcal{P}_{N-1}^{FB-EP}$ or returns a hyperplane that separates p from $\mathcal{P}_{N-1}^{FB-EP}$.

The resulting algorithm can be proven to terminate finitely with the optimal market clearing solution or an infeasibility certificate, by the same arguments used to prove the finite termination of Alg. 1.

4. Simulation setup

In the case study of the following section, we simulate a generalization of the day-ahead markets for LMP, FBMC and ATCMC that were presented in section 2. The generalized formulations additionally consider commitment (on-off) decisions for slow generators[4], reserves, European pricing restrictions for non-divisible bids that correspond to the commitment of resources and the N-1 security criterion. We assume co-optimization of energy and reserve in the day-ahead market, which

differs from the current implementation of the market in Europe where the reserve market can be cleared before, simultaneously, or after the energy market. We adopt this assumption in order to focus on quantifying the impact of zonal pricing on unit commitment. The assumption corresponds to a best-case version of the commitment of reserve.

We simulate real-time markets for managing congestion and balancing the system after renewable energy forecast errors and transmission and generation outages have been revealed. Real-time markets must respect the commitment of slow generators which is decided in the day-ahead market. Moreover, in the case of zonal markets, real-time balancing strives to maintain the cleared net position of each zone. As mentioned in the introduction, these real-time models also correspond to optimistic versions of current European practices in which congestion management and balancing are performed separately. The reader is referred to EC.2 for a detailed presentation of these two-settlement models.

We use a modified version of the CWE instance of Aravena and Papavasiliou (2017) consisting of: (i) 346 slow generators with a total capacity of 154 GW; (ii) 301 fast thermal generators with a total capacity of 89 GW; (iii) 1312 renewable generators with a total capacity of 149 GW; (iv) 632 buses; and (v) 945 branches (3 491 individual circuits[5]). The average demand of the system amounts to 134 GW.

We consider 768 typical snapshots for day-ahead market clearing. Each snapshot corresponds to different demand, renewable forecasts and maintenance schedules (deratings) for thermal generators. For each snapshot, we generate 1 150 random realizations of uncertainty (renewable forecast errors, forced outages of thermal generators and forced outages of transmission lines) in order to simulate real-time operation. For generators and lines, forced outages are randomly generated based on Bernoulli distributions, i.e. each element is completely unavailable with a probability equal to its forced outage rate, otherwise the element is fully available (up to derating from maintenance schedules). In total, we consider 883 200 different operating conditions for each policy. Considering that each snapshot corresponds to an hour of operation, our simulations correspond to approximately 100 years of operation.

Policy	Day-ahead [M€/year]	Real-time [M€/year]	Total [M€/year]	Efficiency losses
Perfect Foresight	–	11 476	11 476	-2.90%
LMP	11 284	534	11 818	–
FBMC	10 458	1 963	12 420	5.09%
ATCMC	10 470	1 949	12 419	5.08%

Table 3 Total costs and cost performance comparison between policies. Efficiency losses measured with respect to LMP total cost.

5. Results and discussion

We present a comparison between LMP, FBMC and ATCMC in terms of their day-ahead and real-time performance. Table 3 presents the overall costs of each policy at each stage. The table also contains the Perfect Foresight (PF) benchmark, which is an unreachable performance benchmark. PF and LMP show important cost differences mainly due to (i) the ability of PF to adapt the commitment of slow units between different realizations of uncertainty and (ii) out-of-merit commitment decisions made by LMP in order to satisfy the N-1 security criterion. In particular, LMP spreads out production through the system in order to obtain nodal net injections that are feasible against any single-element transmission contingency, leading to commitment decisions that are inefficient for scenarios with zero or many simultaneous outages.

LMP exhibits larger day-ahead costs than the zonal designs FBMC and ATCMC, which attain very similar costs at all stages (differences between FBMC and ATCMC are within the termination gap of the corresponding day-ahead models). At the same time, the real-time costs of FBMC and ATCMC are notably greater than those of LMP. As indicated in Fig. 4, this difference stems mostly from the use of fast thermal generators (e.g. gas and oil) in real time by FBMC and ATCMC. The inefficient deployment of these units drives the difference in cost performance between zonal and nodal markets to about 5.1% of the total operation costs (which corresponds to approximately 600 M€/year for the CWE).

In addition to achieving a similar cost performance, FBMC and ATCMC result in similar acceptance/rejection decisions and implied flows. This is indicated in Fig. 5. The center and right box

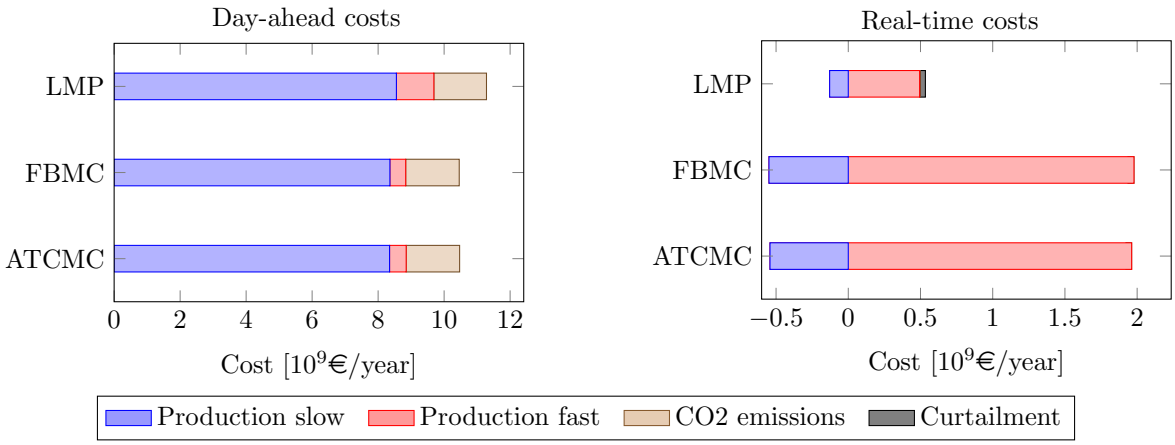

Figure 4 Breakdown of costs in day-ahead market and real-time operations for the three policies under investigation. Real-time costs only account for the differences with respect to day-ahead values.

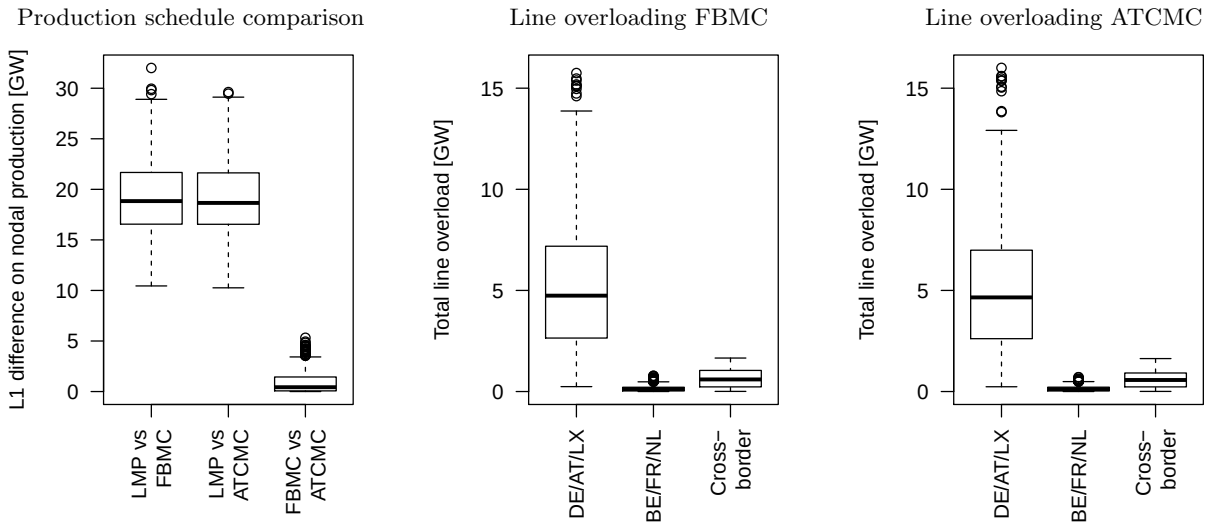

Figure 5 The left box plot presents the distribution of the absolute deviation between the day-ahead production schedules of the three different policies over all snapshots. The center and right box plots present the overloading pattern caused by the acceptance/rejection decisions of FBMC and ATCMC.

plots of Fig. 5 demonstrate that FBMC and ATCMC overload both internal and inter-zonal lines, with similar overloading patterns. This behavior was already observed in the 4-node network in Tables 1 and 2, and is attributed to the fact that zonal merit order dispatch results in similar nodal injections in both models. Zonal merit order overlooks the implications of nodal injections on power flows, thereby failing at allocating transmission capacity.

The differences between FBMC and LMP are driven by the same factors that drive the differences between ATCMC and LMP that are observed in the literature (Ehrenmann and Smeers 2005, Aravena and Papavasiliou 2017). The major factor contributing to the inefficiency of FBMC is the suboptimal commitment decisions of this policy. In order to isolate this factor, we simulate the real-time market without imposing the requirement of maintaining zonal day-ahead net positions, and record the dual variables of the power balance constraints ρ^{RT}. We observe in Fig. 6 that in the majority of cases where LMP commits a unit at a certain location n in the day ahead and FBMC does not, ρ_n^{RT} becomes larger than the corresponding day-ahead zonal price $\rho_{z(n)}^{DA}$, indicating the need for generation at n. On the other hand, whenever FBMC commits at a certain location n in the day ahead and LMP does not, we observe that ρ_n^{RT} can be smaller or larger than $\rho_{z(n)}^{DA}$, depending on forecast errors and forced outages, indicating that generation capacity is not systematically required at the given location. FBMC fails at recognizing these locational differences as a direct consequence of the zonal aggregation in the day-ahead market. We quantify the efficiency losses of FMBC caused by suboptimal commitment at 3.05% of the total operation costs. The remaining 2.04% cost difference is explained by the requirement of maintaining day-ahead net positions in the presence of renewable forecast errors in FBMC, whereas LMP is able to exploit cross-zonal balancing.

6. Conclusions

We present models for flow-based market coupling and for available-transfer-capacity market coupling that do not depend on discretionary parameters and are based purely on the technical parameters of the grid. We analyze the implications of these models on a 4-node instance and a realistic-scale instance of the CWE system. In both instances, we observe that both zonal market designs encounter challenges in allocating the transmission capacity of inter-zonal lines and intra-zonal lines due to the loss of locational information.

These deficiencies affect the real-time performance of the system, leading to efficiency losses of 5.09% for flow-based market coupling and 5.08% for available-transfer-capacity market coupling

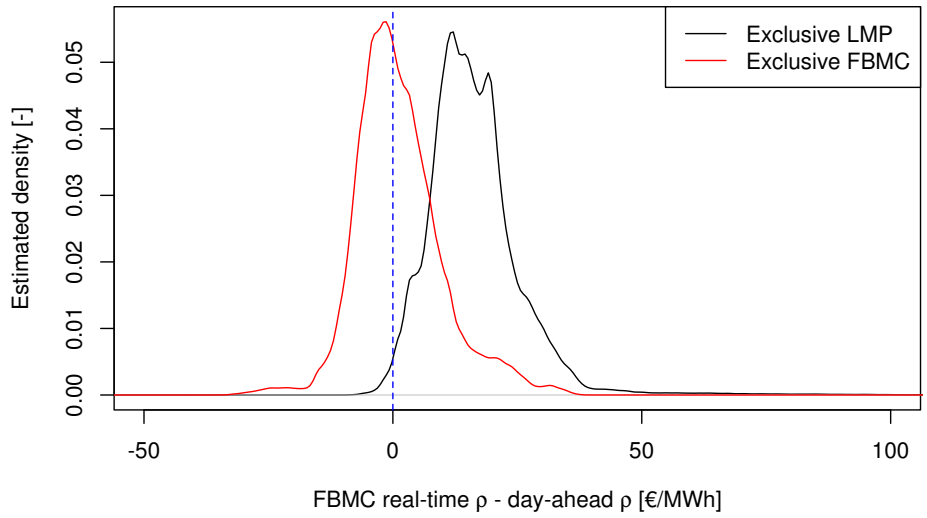

Figure 6 Distribution of geographical averages of marginal cost differences between real time and day ahead for FBMC, without enforcing zonal net positions in real time. For a given snapshot and a given realization of uncertainty, the "exclusive LMP" series is computed by averaging the differences $\rho_n^{RT} - \rho_{z(n)}^{DA}$ over all nodes where LMP committed slow units and FBMC did not commit units, weighted by the capacity committed exclusively by LMP. The exclusive FBMC series is computed analogously.

with respect to a nodal market design. The similarities that are unveiled between both zonal designs raise the question of whether flow-based market coupling should be expanded to cover other zones of Europe, especially when certain zones such as Poland are already planning to switch to a nodal market design (PSE S.A. 2017).

Future extensions of the present work will focus on the impact of the flow-based model with exact projection on prices and on the study of the meaning of these prices as they relate to investment.

Endnotes

[1]The Flow Reliability Margin is a parameter that is used by TSOs in order to decrease the capacity of critical branches that are offered to the market. The role of flow reliability margins is to account for uncertainties during the capacity calculation process (i.e. uncertainties linked to the definition of the base case or to the simplified network representation).

[2]In what concerns the firmness of cross-border capacity, we note that the new Regulation (EU) 2019/943 requires instead that 70% of the capacity of the lines be made available to the market, even if this implies using cross-border redispatch in order to support the cleared net positions. An analysis of the implications of this new rule is outside the scope of the present paper. Instead, we consider in this paper the principle of firmness of cross-border capacity, as described in Regulation (EU) 2015/1222.

[3]The influence of N-1 security on the FBMC model used in the day-ahead European market clearing model can be appreciated when analysing historical data of the flow-based constraints that are used as input for the market coupling process. These constraints are publicly available online: `https://www.jao.eu/`. At the time of writing (February 11, 2020), 89% of the constraints were associated to a contingency. Another evidence of the importance of the security criterion for providing results with policy relevance can be found in the first edition of the bidding zone review (ENTSO-E 2018). In the review, the participants mention the absence of N-1 security as a reason for the failure of the model-based bidding zone configuration proposals.

[4]We refer to slow generators as generators with a unit commitment schedule that needs to be fixed in the day-ahead time frame and cannot be changed in real time. Concretely, these correspond to coal and nuclear units.

[5]Each N-1 transmission contingency corresponds to the forced outage of a single circuit.

References

50Hertz, Amprion, APG, Creos, Elia, EPEXSpot, RTE, TenneT, Transnet BW (2017) Documentation of the CWE FB MC solution.

ACER (2018) Annual report on the results of monitoring the internal electricity and natural gas markets in 2017.

ACER (2019) Monitoring report on the implementation of the cacm regulation and the fca regulation.

Amprion, APG, Creos, Elia, RTE, TenneT, Transnet BW (2015) CWE flow based market-coupling project: Parallel run performance report.

APX Group, Belpex, Cegedel Net, EEX, ELIA Group, EnBw, E-On Netz, Powernext, RTE, RWE, TenneT (2010) A report for the regulators of the Central West European (CWE) region on the final design of the market coupling solution in the region, by the CWE MC Project. (Avalaible at: http://www.epexspot.com/en/market-coupling/documentation_cwe).

APX Group, Belpex, Powernext (2006) Trilateral Market Ccoupling algorithm.

Aravena I, Papavasiliou A (2017) Renewable energy integration in zonal markets. *IEEE Transactions on Power Systems* 32(2):1334–1349, ISSN 0885-8950.

Ben-Tal A, El Ghaoui L, Nemirovski A (2009) *Robust Optimization*. Princenton Series in Applied Mathematics (Princeton University Press), ISBN 9781400831050.

Boyd S, Vandenberghe L (2004) *Convex Optimization* (Cambridge University Press).

CAISO (2015) Business Practice Manual for Market Operations (version 45).

Comission FER (2018) Market Oversight, Electric Power Markets. URL `https://www.ferc.gov/market-oversight/mkt-electric/overview.asp`, accessed: 2018-04-26.

CREG (2017) Functioning and design of the Central West European day-ahead flow based market coupling for electricity: Impact of TSOs discretionary actions.

Dierstein C (2017) Impact of generation shift key determination on flow based market coupling. *2017 14th International Conference on the European Energy Market (EEM)*, 1–7.

Ehrenmann A, Smeers Y (2005) Inefficiencies in European congestion management proposals. *Utilities Policy* 13(2):135 – 152, ISSN 0957-1787.

Energy Markets Inspectorate (EI, Sweden), Norwegian Water Resources and Energy Directorate (NVE) (2017) Reduced capacity on German-Nordic interconnectors, regulatory framework and socioeconomic effects on the European electricity market.

ENTSO-E (2018) First edition of the bidding zone review - final report.

European Commission (2015) Commission Regulation (EU) 2015/1222 of 24 July 2015 establishing a guideline on capacity allocation and congestion management.

European Commission (2017a) Commission Regulation (EU) 2017/1485 of 2 August 2017 establishing a electricity transmission system operation.

European Commission (2017b) Commission Regulation (EU) 2017/2195 of 23 November 2017 establishing a guideline on electricity balancing.

European Network of Transmission System Operators for Electricity (ENTSO-E) (2017) Statistical Factsheet 2016.

European Network of Transmission System Operators for Electricity (ENTSO-E) (2018) ENTSO-E transparency platform. URL `https://transparency.entsoe.eu/`, accessed: 2018-04-26.

European Parliament, Council of the European Union (2003) Regulation 1228/2003 of the European Parliament and of the Council of 26 June 2003 on conditions for access to the network for cross-border exchanges in electricity.

European Parliament, Council of the European Union (2009) Regulation (EC) No 714/2009 of the European Parliament and of the Council of 13 July 2009 on conditions for access to the network for cross-border exchanges in electricity and repealing Regulation (EC) No 1228/2003.

Eurostat (2018) Population on 1 January. URL `http://ec.europa.eu/eurostat/tgm/table.do?language=en&pcode=tps00001`, accessed: 2018-04-26.

Grid Optimization Competition (2018) SCOPF Problem Formulation: Challenge 1. URL `https://gocompetition.energy.gov/challenges/challenge-1/formulation`, accessed: 2018-11-29.

Hogan WW (2016) Virtual bidding and electricity market design. *The Electricity Journal* 29(5):33 – 47, ISSN 1040-6190.

Jensen TV, Kazempour J, Pinson P (2017) Cost-optimal atcs in zonal electricity markets. *IEEE Transactions on Power Systems* PP(99):1–1, ISSN 0885-8950.

Joint Allocation Office (2015) Yearly long term auctions. URL `http://www.jao.eu/marketdata/yearlylongtermauctions`.

Marien A, Luickx P, Tirez A, Woitrin D (2013) Importance of design parameters on flowbased market coupling implementation. *2013 10th International Conference on the European Energy Market (EEM)*, 1–8, ISSN 2165-4077.

McCormick GP (1976) Computability of global solutions to factorable nonconvex programs: Part I — convex underestimating problems. *Mathematical Programming* 10(1):147–175, ISSN 1436-4646.

Papavasiliou A, Smeers Y, de Maere d'Aertrycke G (2019) Study on the general design of a mechanism for the remuneration of reserves in scarcity situations. URL `https://perso.uclouvain.be/anthony.papavasiliou/public_html/CREGReportFinal.pdf`.

PSE SA (2017) PSE S.A. informs on the conclusion of the tendering procedure for the supply and implementation of the Electricity Balancing Market Management System in Poland. URL `https://www.pse.pl/web/pse-eng/-/pse-s-a-informs-on-the-conclusion-of-the-tendering-procedure-for-the-supply-and-implementation-of-the-electricity-balancing-market-management-system-i`.

RTE (2006) Réferentiel Technique.

Schweppe F, Caramanis M, Tabors R, Bohn R (1988) *Spot Pricing of Electricity*. Power Electronics and Power Systems (Springer US), ISBN 9780898382600.

Street A, Moreira A, Arroyo JM (2014) Energy and reserve scheduling under a joint generation and transmission security criterion: An adjustable robust optimization approach. *IEEE Transactions on Power Systems* 29(1):3–14, ISSN 0885-8950.

TenneT (2014) Determining securely available cross-border transmission capacity.

Van den Bergh K, Boury J, Delarue E (2016) The flow-based market coupling in central western europe: Concepts and definitions. *The Electricity Journal* 29(1):24 – 29, ISSN 1040-6190.

Waniek D, Rehtanz C, Handschin E (2010) Flow-based evaluation of congestions in the electric power transmission system. *2010 7th International Conference on the European Energy Market*, 1–6, ISSN 2165-4077.

This page is intentionally blank. Proper e-companion title page, with INFORMS branding and exact metadata of the main paper, will be produced by the INFORMS office when the issue is being assembled.

Appendix to: Transmission capacity allocation in zonal electricity markets

This electronic companion is organized as follows. Section EC.1 presents proofs for the propositions in section 3 of the main document and an algorithm for computing available transfer capacities considering the N-1 criterion. Section EC.2 presents market models that extend the models introduced in section 2 of the main document. These extended models account for day-ahead and real-time markets, reserves, commitment decisions and European linear pricing restrictions. Section EC.3 explains how European linear pricing restrictions, introduced in section EC.2, can be derived by adapting the duality framework of Madani and Van Vyve (2015). Section EC.4 finalizes the document by providing additional details about our case study and simulations.

EC.1. Proofs and additional algorithms for section 3

EC.1.1. Proofs for propositions of section 3

The proof of Prop. 1 relies on the application of known results on convex analysis and cutting plane algorithms to Alg. 1.

PROPOSITION EC.1. *$d(r, \mathcal{R}_{N-1})$ is a piecewise linear convex function of r with finitely many pieces.*

Proof of Prop. EC.1. The convexity of $d(r, \mathcal{R}_{N-1})$ in r follows from the fact that it is the maximum over linear functions of r (Boyd and Vandenberghe 2004), which also implies that $d(r, \mathcal{R}_{N-1})$ is piecewise linear. The function $d(r, \mathcal{R}_{N-1})$ can be described using finitely many pieces because, for each fixed feasible u, the feasible set of the remaining variables in (18) is a polytope, and polytopes can be described using finitely many extreme points and extreme rays. □

PROPOSITION 1. *Algorithm 1 terminates with an optimal solution in a finite number of iterations when using IOD as an injection oracle.*

Proof of Prop. 1. The proof is identical to the proof of convergence of Benders decomposition for linear programs, see Benders (1962). Essentially, due to Prop. EC.1 there exists only a finite number of separating hyperplanes that can be generated using the oracle. Once all these separating

hyperplanes have been generated, the market clearing oracle will solve the original clearing problem (14) – (16), terminating either with the optimal solution or with an infeasibility certificate. □

The cutting-plane algorithm for FBMC under N-1 security can be proven to converge finitely by identical arguments to those presented in the proofs of Prop. EC.1 and Prop. 1.

In contrast with the previous propositions, which focus on convergence results, the following proposition focuses on the limits for inter-zonal exchanges in different policies. Specifically, Prop. 2 states that, under the N-1 security criterion, inter-zonal exchanges are more restricted in LMP than in FBMC.

PROPOSITION 2. *Let $\mathcal{P}^{LMP}_{N-1}$ be the feasible set of zonal net positions of the nodal market under N-1 security, i.e. the projection of $\{(v,r)\in[0,1]^{|G|}\times\mathbb{R}^{|N|} \mid (15),(16)\}$ onto the zonal net position space. Then $\mathcal{P}^{LMP}_{N-1}\subseteq\mathcal{P}^{FB-EP}_{N-1}$.*

Proof of Prop. 2. The proof proceeds by comparing the descriptions of $\mathcal{P}^{LMP}_{N-1}$ and $\mathcal{P}^{FB-EP}_{N-1}$ when considering explicitly all transmission contingencies. Let $I:=\{0\}\cup L$ be the base case and contingency cases of the system, and $1_{l,i}=1$ if $l\neq i$ and $1_{l,i}=0$ otherwise. Then, we can describe $\mathcal{P}^{LMP}_{N-1}$ as follows:

$$
\begin{aligned}
\mathcal{P}^{LMP}_{N-1} = \Bigg\{ p\in\mathbb{R}^{|Z|} \;\Bigg|\; & \exists (v,r)\in[0,1]^{|G|}\times\mathbb{R}^{|N|}: \sum_{n\in N(z)} r_n = p_z \;\forall z\in Z, \\
& r_n = \sum_{g\in G(n)} Q_g v_g - Q_n \;\forall n\in N,\; r\in \cap_{\substack{u\in\{0,1\}^{|L|}\\ \|u\|_1\leq 1}} \mathcal{R}(u) \Bigg\} \\
= \Bigg\{ p\in\mathbb{R}^{|Z|} \;\Bigg|\; & \exists (v,r,f,\theta)\in[0,1]^{|G|}\times\mathbb{R}^{|N|}\times\mathbb{R}^{|L|\cdot|I|}\times\mathbb{R}^{|N|\cdot|I|}: \\
& \sum_{n\in N(z)} r_n = p_z \;\forall z\in Z,\; r_n = \sum_{g\in G(n)} Q_g v_g - Q_n \;\forall n\in N, \\
& r_n = \sum_{l\in L(n,\cdot)} f_{l,i} - \sum_{l\in L(\cdot,n)} f_{l,i} \;\forall n\in N, i\in I, \\
& -F_l \leq f_{l,i}\leq F_l,\; f_{l,i} = B_l\cdot 1_{l,i}\cdot\left(\theta_{m(l),i}-\theta_{n(l),i}\right) \quad \forall l\in L, i\in I \Bigg\}.
\end{aligned}
$$

In the same fashion, we can describe $\mathcal{P}^{FB-EP}_{N-1}$ as:

$$\mathcal{P}^{FB-EP}_{N-1} = \Bigg\{ p \in \mathbb{R}^{|Z|} \;\Bigg|\; \exists (v,r,f,\theta) \in [0,1]^{|G|\cdot|L|} \times \mathbb{R}^{|N|\cdot|I|} \times \mathbb{R}^{|L|\cdot|I|} \times \mathbb{R}^{|N|\cdot|I|} :$$

$$\sum_{n \in N(z)} r_{n,i} = p_z \;\forall z \in Z, i \in I,\; r_{n,i} = \sum_{g \in G(n)} Q_g v_{g,i} - Q_n \;\forall n \in N, i \in I,$$

$$r_{n,i} = \sum_{l \in L(n,\cdot)} f_{l,i} - \sum_{l \in L(\cdot,n)} f_{l,i} \;\forall n \in N, i \in I,$$

$$-F_l \leq f_{l,i} \leq F_l,\; f_{l,i} = B_l \cdot 1_{l,i} \cdot \left(\theta_{m(l),i} - \theta_{n(l),i}\right) \quad \forall l \in L, i \in I \Bigg\}.$$

The equations describing $\mathcal{P}^{FB-EP}_{N-1}$ are a relaxation of the equations describing $\mathcal{P}^{LMP}_{N-1}$, therefore $\mathcal{P}^{LMP}_{N-1} \subseteq \mathcal{P}^{FB-EP}_{N-1}$. $\square$

The result of Prop. 2 contrasts with the analogous comparison in absence of the N-1 security criterion, where $\mathcal{P}^{LMP} = \mathcal{P}^{FB-EP}$. The root of this difference is the loss of locational information in FBMC. A zonal net position can correspond to many nodal net injections, hence a zonal net position might respect the N-1 security criterion on FBMC by resorting to different nodal net injections on each contingency. On the contrary, a nodal net injection respects the N-1 security criterion on LMP only if it can be maintained across contingencies.

EC.1.2. Decomposition algorithm for computing maximum-volume Available-Transfer-Capacities with N-1 security

Our approach for computing maximum-volume ATCs under N-1 security is analogous to the approach presented in subsection 3.2 for solving the FBMC clearing problem. We solve the ATC computation problem,

$$\max_{ATC} \prod_{t \in T} \left(ATC^-_t + ATC^+_t\right)$$

$$\text{s.t.} \quad -ATC^-_t \leq ATC^+_t \quad \forall t \in T$$

$$[-ATC^-, ATC^+] \subseteq \mathcal{E}^{EP}_{N-1},$$

where $\mathcal{E}^{EP}_{N-1}$ is the set of feasible bilateral exchanges under N-1 security, by replacing the inclusion constraint $[-ATC^-, ATC^+] \subseteq \mathcal{E}^{EP}_{N-1}$ with a set of linear inequalities that are generated iteratively.

Geometrically, our algorithm constructs an outer approximation of $\mathcal{E}^{EP}_{N-1}$ via linear inequalities, so that a maximum-volume rectangle inscribed in the outer approximation is also a maximum-volume rectangle inscribed in $\mathcal{E}^{EP}_{N-1}$.

Following the notion of N-1 security for zonal markets presented in subsection 3.2, we formally define $\mathcal{E}^{EP}_{N-1}$ as the set of all possible bilateral exchanges that can be achieved with N-1 secure net positions, that is $\mathcal{E}^{EP}_{N-1} = \left\{e \in [-E, E] \middle| \exists p \in \mathcal{P}^{FB-EP}_{N-1}, p = -Qe\right\}$, where $E_t = \sum_{l \in L(t)} F_l$ for all $t \in T$ and Q is the incidence matrix of the graph defined by the zones Z (vertices) and the interconnectors T (edges). Observe that $\mathcal{E}^{EP}_{N-1}$ is a convex polytope because it is constructed as an affine transformation of $\mathcal{P}^{FB-EP}_{N-1}$ intersected with a box. Therefore, we can describe $\mathcal{E}^{EP}_{N-1}$ using finitely many inequalities, i.e. for certain $A \in \mathbb{R}^{M \times |T|}$, $B \in \mathbb{R}^M$ we have $Ae \leq B \iff e \in \mathcal{E}^{EP}_{N-1}$. While A, B are not available, we can construct them iteratively. This line of reasoning leads to Alg. 2, which starts from a box outer approximation of $\mathcal{E}^{EP}_{N-1}$ and iteratively refines the approximation by means of two oracles:

- A maximum volume oracle $MVO(A, B)$ which, for given $A \in \mathbb{R}^{M \times |T|}$ and $B \in \mathbb{R}^M$, finds a maximum-volume rectangle inscribed in $\{e \in \mathbb{R}^{|T|} \mid Ae \leq B\}$ and returns ATC^{-*}, ATC^{+*}. In other words, the maximum volume oracle solves the following convex mathematical program

$$\max_{ATC} \sum_{t \in T} \log\left(ATC^-_t + ATC^+_t\right)$$
$$\text{s.t. } A^+ ATC^+ - A^- ATC^- \leq B,$$

where $a^+_{ij} = \max\{0, a_{ij}\}$ and $a^-_{ij} = \min\{0, a_{ij}\}$ (Boyd and Vandenberghe 2004).

- An exchange oracle $EO(ATC^-, ATC^+)$ which, for given ATCs, ATC^-, ATC^+, either certifies that $[-ATC^-, ATC^+] \subseteq \mathcal{E}^{EP}_{N-1}$ or returns a hyperplane, defined in terms of slope $a \in \mathbb{R}^{|T|}$ and intercept $b \in \mathbb{R}$. This hyperplane separates a subset of $[-ATC^-, ATC^+]$ from $\mathcal{E}^{EP}_{N-1}$.

As in the case of the algorithm for LMP, the challenge in attaining practical performance with Alg. 2 is in designing an effective exchange oracle. An exchange oracle that checks independently all vertices of the rectangle $[-ATC^-, ATC^+]$ for all possible contingencies would consume a prohibitive amount of time at each iteration, thereby rendering Alg. 2 ineffective. Instead, we can check all

Algorithm 2 Cutting-plane algorithm for maximum-volume ATCs.

1: Initialize $A := [I_{|T|\times|T|} \ -I_{|T|\times|T|}]^\top, B := [E^\top \ E^\top]^\top$, `inclusion` := `FALSE`
2: **while** !`inclusion` **do**
3: Call $MVO(A,B) \to ATC^-, ATC^+$
4: Call $EO(ATC^-, ATC^+) \to$ `inclusion`, (a,b)
5: $A := [A^\top \ a]^\top, \ B := [B^\top \ b]^\top$
6: **end while**
7: Terminate: ATC^-, ATC^+ are maximum-volume ATCs.

these combinations implicitly within a single mathematical program. In order to construct such a mathematical program, we note the following. Firstly,

$$[-ATC^-, ATC^+] \subseteq \mathcal{E}^{EP}_{N-1} \iff d(-Qe, \mathcal{P}^{FB-EP}_{N-1}) = 0 \ \ \forall e \in [-ATC^-, ATC^+],$$

where $d\left(p, \mathcal{P}^{FB-EP}_{N-1}\right)$ is defined according to (19). This distance can be expressed equivalently as

$$\begin{aligned} d(\bar{p}, \mathcal{P}^{FB-EP}_{N-1}) \ = \max_{u,\psi,\sigma,\gamma,\phi,\rho} \ & \sum_{z\in Z} \bar{p}_z \psi_z + \sum_{n\in N} Q_n \rho_n + \sum_{z\in Z} \psi_z \cdot \sum_{n\in N(z)} Q_n - \sum_{g\in G} \sigma_g - \sum_{l\in L} F_l(\gamma_l^- + \gamma_l^+) \\ \text{s.t.} \ & -1 \le \psi_z \le 1 \quad \forall z \in Z \\ & \sigma_g \ge Q_g(1-u_g)(\rho_{n(g)} + \psi_{z(g)}) \quad \forall g \in G \\ & -\gamma_l^- + \gamma_l^+ + \phi_l - \rho_{n(l)} + \rho_{m(l)} = 0 \quad \forall l \in L \\ & \sum_{l\in L(n,\cdot)} B_l(1-u_l)\phi_l + \sum_{l\in L(\cdot,n)} B_l(1-u_l)\phi_l = 0 \quad \forall n \in N \\ & \sigma \ge 0, \gamma \ge 0, u \in \{0,1\}^{|G|+|L|}, \|u\|_1 \le 1. \end{aligned} \tag{EC.1}$$

Secondly, $-E \le -ATC^- \le ATC^+ \le E$ by construction of Alg. 2. Furthermore, by convexity of $\mathcal{P}^{FB-EP}_{N-1}$, $d(Qe, \mathcal{P}^{FB-EP}_{N-1}) = 0$ for e at all the vertices of $[-ATC^-, ATC^+]$ is a necessary and sufficient condition for $[-ATC^-, ATC^+] \subseteq \mathcal{E}^{EP}_{N-1}$. Then, we can generate valid separating hyperplanes using the following function:

$$\Delta\left(ATC^-, ATC^+\right) = \max_{s\in\{0,1\}^{|T|}} d(-Q(-ATC^- + s \odot (ATC^+ + ATC^-)), \mathcal{P}^{FB-EP}_{N-1}), \tag{EC.2}$$

where $\odot$ denotes the Hadamard product (element-wise multiplication of vectors). The function $\Delta\left(ATC^-, ATC^+\right)$ corresponds to the maximum distance between (i) the zonal net position at any

vertex of $[-ATC^-, ATC^+]$ and (ii) the feasible set of net positions. The function $\Delta\left(ATC^-, ATC^+\right)$ is a convex function, as shown in the following result.

PROPOSITION EC.2. *The function $\Delta(ATC^-, ATC^+)$ is a piecewise linear convex function of ATC^-, ATC^+ with finitely many pieces.*

Proof of Prop. EC.2. To see that $\Delta(ATC^-, ATC^+)$ is a piecewise linear convex function of ATC^-, ATC^+, simply replace the definition of $d(p, \mathcal{P}_{N-1}^{FB-EP})$ given in (EC.1) into (EC.2) and fuse both max operators ($\Delta(ATC^-, ATC^+)$ is a max-type function over an objective which is linear in ATC^-, ATC^+ (Boyd and Vandenberghe 2004)). The proof that $\Delta(ATC^-, ATC^+)$ has finitely many pieces follows the same argument as the one used in the proof of Prop. EC.1. □

We then propose an exchange oracle based on Δ, abbreviated as EOD, which performs the following operations at every query point ATC^-, ATC^+:

1. Compute $\tilde{b} := \Delta(ATC^-, ATC^+)$ and record s^*, ψ^* (see (EC.1), (EC.2)).
2. If $\tilde{b} = 0$, then return `TRUE`, $(0_{|T|}, 0)$.
3. Else return `FALSE`, $(-\psi^{*\top} Q, -\tilde{b} - \psi^{*\top} Q(-A\bar{T}C^- + s^* \odot (ATC^+ + ATC^-)))$.

Using this exchange oracle in Alg. 2 we can show the following:

PROPOSITION EC.3. *Algorithm 2 terminates with an optimal solution in a finite number of iterations when using EOD as exchange oracle.*

Proof of Prop. EC.3. Identical to the proof of Prop. 1, using the result of Prop. EC.2. □

Finally, note that the underlying mathematical problem for computing $\Delta(ATC^-, ATC^+)$ can be cast as a bi-linear program, where products between variables can be replaced by their McCormick envelopes. The function $\Delta(ATC^-, ATC^+)$ can, therefore, be evaluated by solving a mixed integer linear program.

EC.2. Two-settlement market clearing models

In this section we extend the models presented in section 2 to a two-stage setting where the first stage takes place in the day ahead and consist of clearing energy and reserve markets simultaneously,

while the second stage takes place in real time and corresponds to the actual operation of the system. Multi-settlement systems allow market participants to update their positions in the market as new information becomes available. In the context of electricity markets, new information can come from improved modeling of the grid (Kamat and Oren 2002, 2004), changes in forecasts of renewable production or demand, and forced outages.

While it is not the case in general, certain multi-settlement systems can create systematic arbitrage opportunities, allowing market participants to earn a profit without actually producing/consuming in real time. Multi-settlement zonal electricity markets, in particular, can and have been gamed, perhaps most notoriously by the use of the *dec-game* by participants of the California Power Exchange in the early 2000's (FERC 2007). These effects have also been studied in the literature using game theoretic models and small network examples (Kamat and Oren 2002, 2004). In this work, in order to permit the simulation of realistic systems, and as stated in section 2, we assume that participants do not game the transmission markets and that, instead, they act as price takers, by submitting their real costs to the corresponding auctions. We ignore inter-temporal constraints and we model only 1-hour snapshots. We use the two-settlement system presented in Fig. EC.1. For both day-ahead and real-time market models, we consider 3 types of market participants:

1. Consumers, who submit continuous bids for energy Q_c, P_c (demand response) to both day-ahead and real-time markets.

2. Fast generators, i.e. generators that can be started on short notice. These resources submit continuous bids for energy $Q_i, P_i, \forall i \in I(g)$ to both day-ahead and real-time markets, and submit their reserve capability Q_g^R to the day-ahead market.

3. Slow generators, i.e. thermal generators that can only be started on a 24-hour or longer notice. In the day-ahead market, slow generators submit a linked family of bids consisting of (i) a block bid associated with their minimum production level Q_g^L, K_g, (ii) continuous bids for energy $Q_i, P_i, \forall i \in I(g)$ and (iii) their reserve capability Q_g^R. These continuous bids for energy and reserve can only be accepted if the block bid is accepted. In the real-time market, slow generators submit continuous bids for energy only if they are committed in the day-ahead market.

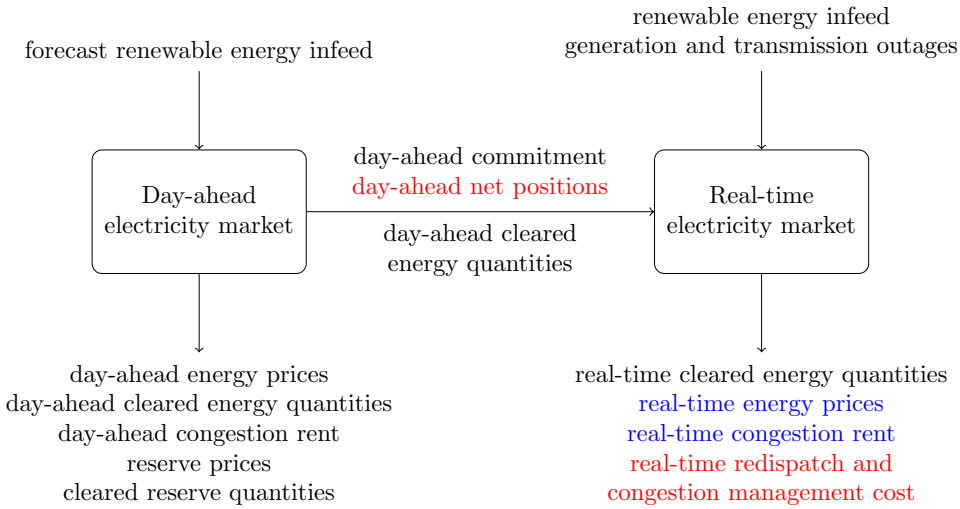

Figure EC.1 Block diagram of the two-settlement system used in the paper. The day-ahead market is cleared based on a forecast of the renewable energy infeed, assuming that all generation and transmission elements are available. Reserve margins are imposed in order to cope with uncertainty. The real-time market is cleared using the actual renewable infeed and forced outages of generation and transmission elements. We indicate common features of nodal and zonal electricity markets using black, features that are only present in nodal markets using blue, and features that are only present in zonal markets using red.

We compute day-ahead prices following the rules of European electricity markets for continuous bids and linked families of bids (EPEX Spot et al. 2016, Madani and Van Vyve 2015), with two adaptations: we model the clearing of energy and reserves simultaneously, and we allow continuous bids to be children within linked bid families. These rules and adaptations result in the following restrictions over day-ahead prices:

1. Continuous bids must be accepted if they are in-the-money, must be rejected if they are out-of-the-money, and can be partially accepted only if they are at-the-money.

2. Linked families can be accepted only if the linked family is in-the-money or at-the-money. A continuous bid i within a linked family must respect restriction 1, conditional on the acceptance of its parent $g(i)$, i.e. i must follow restriction 1 if $g(i)$ is accepted and i must be rejected if $g(i)$ is rejected (even if it is in-the-money).

Considering these features, along with the N-1 security criterion (described in sections 3 and EC.1) and the features presented in Fig. EC.1, we clear day-ahead markets by solving mixed-integer linear programs and real-time markets by solving linear programs. The set of features modeled in the present study have not been simultaneously accounted for neither by industrial studies (Amprion et al. 2015) nor by previous academic studies on the subject (Waniek et al. 2009), (Waniek et al. 2010, Marien et al. 2013, Dierstein 2017). In what follows, we first list the nomenclature used in the clearing models, and then we introduce the nodal electricity market model and the zonal electricity market models.

Nomenclature

Sets

G	generators
I	production continuous bids
C	consumers
N	buses
L	lines
Z	bidding zones
T	interconnectors
R	reserves
$G(n), G(z)$	generators at node n, zone z
$G(r)$	generators providing reserve r
$I(n), I(z)$	production bids at bus n, zone z
$I(g)$	production bids of generator g
$C(n), C(z)$	consumers at bus n, zone z
$L(m,n)$	lines from bus m to bus n
$T(y,z)$	interconnectors from zone y to zone z
G^{SLOW}	slow generators
G^{FAST}	fast generators
L^{RT}	lines available in real time

Parameters

$P_\cdot, Q_\cdot$	price-quantity pair for a bid
$P_\cdot^{RT}, Q_\cdot^{RT}$	price-quantity pair for a bid in real time
K_g, Q_g^L	cost and quantity of block bid for technical minimum of generator g
$Q_g^{L,RT}$	post-contingency quantity of block bid of generator g
Q_g^R	reserve capability, generator g
Q_g^U	total capacity, generator g
F_l, B_l	thermal capacity and susceptance of line l
$z(g), n(g)$	zone and node corresponding to generator g
$r(g)$	reserve of generator g
$z(c), n(c)$	zone and node of consumer c
$m(l), n(l)$	node from and node to line l
$a(t), b(t)$	zone from and zone to interconnector t

$V_{f,n}, V_{f,z}$	left-hand-side coefficients of transmission constraint f
W_f	right-hand-side coefficient of transmission constraint f

Variables

u_g	acceptance of block bid of generator g
v_i	acceptance of production bid i
w_g	acceptance of reserve procurement by generator g
x_c	acceptance of demand response bid c
y_r	acceptance of reserve response bid r
r_n	net injection at bus n
p_z	net position of zone z
e_t	exchange through interconnector t
σ_g	surplus of slow generator g
ς_i	surplus of production bid i
ν_g	capacity price of generator g
τ_g	surplus of reserve bid of generator g
σ_c	surplus of demand response bid c
ρ_n, ρ_z	energy price at node n, zone z
π_r	price for reserve r
γ, ϕ	dual variables of transmission constraints

EC.2.1. Two-settlement nodal electricity market models

Two-settlement nodal electricity market models commonly consist of a day-ahead unit commitment model and a real-time optimal power flow model. While the real-time model that we employ is standard in the literature, our day-ahead model includes additional variables and constraints that ensure the existence of prices that respect European electricity market restrictions. These variables and constraints have been derived using duality theory, following the framework of Madani and Van Vyve (2015). In short, they correspond to a modified version of the dual variables and constraints of the linear relaxation of the unit commitment problem. Note, however, that the models proposed in section 2 are general, in the sense that they are not limited by the idiosyncratic pricing rules of European day-ahead electricity markets. The reader is referred to section EC.3 for the full derivation of our day-ahead market clearing models.

EC.2.1.1. Day-ahead market model First, we define sets $\mathcal{D}$ describing the feasible domains for each type of agent. These sets will be common across our different clearing models for the day-ahead market.

The feasible domain for each consumer $c \in C$, presented in (EC.3), allows the energy bid to be partially accepted and ensures that the resulting surplus is non-negative.

$$\mathcal{D}_c := \left\{(x,\sigma,\rho) \in [0,1]\times\mathbb{R}_+\times\mathbb{R} \;\middle|\; \sigma \geq Q_c(\rho - P_c)\right\} \tag{EC.3}$$

Relation (EC.4) defines the feasible domain $\mathcal{D}_g$ for fast generators $g \in G^{FAST}$.

$$\begin{aligned}\mathcal{D}_g := \Bigg\{ & (v,w,\varsigma,\tau,\nu,\rho,\pi) \in [0,1]^{|I(g)|}\times[0,1]\times\mathbb{R}_+^{|I(g)|}\times \\ & \mathbb{R}_+\times\mathbb{R}_+\times\mathbb{R}\times\mathbb{R} \;\Big|\; \varsigma_i \geq Q_i(\rho-\nu-P_i)\ \forall i\in I(g), \\ & \tau \geq Q_g^R(\pi-\nu),\ \sum_{i\in I(g)} Q_i v_i + Q_g^R w \leq Q_g^U \Bigg\}\end{aligned} \tag{EC.4}$$

The set $\mathcal{D}_g, g \in G^{FAST}$, allows for continuous bids for energy and reserve to be partially accepted, it ensures that the associated surplus of each bid is non-negative and that the total capacity accepted does not surpass the maximum capacity of the generator.

The feasible domain $\mathcal{D}_g$ for slow generators $g \in G^{SLOW}$ is defined as follows:

$$\begin{aligned}\mathcal{D}_g := \Bigg\{ & (u,v,w,\sigma,\varsigma,\tau,\nu,\rho,\pi) \in \{0,1\}\times\mathbb{R}_+^{|I(g)|}\times\mathbb{R}_+\times \\ & \mathbb{R}_+\times\mathbb{R}_+^{|I(g)|}\times\mathbb{R}_+\times\mathbb{R}_+\times\mathbb{R}\times\mathbb{R} \;\Big|\; v_i \leq u\ \forall i\in I(g), \\ & w \leq u,\ \varsigma_i \geq Q_i(\rho-\nu-P_i)\ \forall i\in I(g), \\ & \tau \geq Q_g^R(\pi-\nu),\ Q_g^L u + \sum_{i\in I(g)} Q_i v_i + Q_g^R w \leq Q_g^U, \\ & \sigma \geq Q_g^L\rho + \sum_{i\in I(g)}\varsigma_i + \tau - Q_g^L\nu - K_g - M_g(1-u) \Bigg\}\end{aligned} \tag{EC.5}$$

Definition (EC.5) enforces that continuous bids for energy and reserve can be partially accepted only if the parent block bid is accepted ($u = 1$), it ensures that the associated surplus of each continuous bid is non-negative and that the total capacity accepted does not surpass the maximum capacity of the generator. The surplus of the parent block bid σ consists of the surplus of the block bid (Q_g^L, K_g) plus the surplus of the child bids in the linked family ($\varsigma_i\ \forall i \in I(g)$ and τ), i.e. σ accumulates the entire surplus of the linked family. The parameter M_g has to be large enough so that σ can be made zero by setting $u = 0$, even when the family is in-the-money (i.e. when $Q_g^L\rho + \sum_{i\in I(g)}\varsigma_i + \tau - Q_g^L\nu - K_g > 0$).

We model system operators as additional agents that submit bids for reserve response Q_r, P_r for each corresponding control area. The feasible domain for reserves is accordingly defined as

$$\mathcal{D}_r := \Big\{ (w,y,\sigma,\pi) \in \mathbb{R}^{|G(r)|} \times [0,1] \times \mathbb{R}_+ \times \mathbb{R}_+ \;\Big|\; \sum_{g\in G(r)} Q_g^R w_g \geq Q_r(1-y),\ \sigma \geq Q_r(\pi - P_r) \Big\}, \tag{EC.6}$$

where we enforce reserve balance and that the surplus of reserve response bids is non-negative.

Using sets $\mathcal{D}_c, \mathcal{D}_g$ and $\mathcal{D}_r$, the nodal day-ahead market clearing problem can be formulated as (EC.7) – (EC.14).

$$\min_{\substack{u,v,w,x,y,r\\ \sigma,\varsigma,\tau,\nu,\rho,\phi,\gamma,\pi}} \sum_{g\in G^{SLOW}} K_g u_g + \sum_{i\in I} P_i Q_i v_i + \sum_{c\in C} P_c Q_c x_c + \sum_{r\in R} P_r Q_r y_r \tag{EC.7}$$

$$\text{s.t.} \quad \big(u_g, v_{I(g)}, w_g, \sigma_g, \varsigma_{I(g)}, \tau_g, \nu_g, \rho_{n(g)}, \pi_{r(g)}\big) \in \mathcal{D}_g \quad \forall g \in G^{SLOW},$$

$$\big(v_{I(g)}, w_g, \varsigma_{I(g)}, \tau_g, \nu_g, \rho_{n(g)}, \pi_{r(g)}\big) \in \mathcal{D}_g \quad \forall g \in G^{FAST} \tag{EC.8}$$

$$\big(x_c, \sigma_c, \rho_{n(c)}\big) \in \mathcal{D}_c \quad \forall c \in C \tag{EC.9}$$

$$\big(w_{G(r)}, y_r, \sigma_r, \pi_r\big) \in \mathcal{D}_r \quad \forall r \in R \tag{EC.10}$$

$$r_n = \sum_{g\in G^{SLOW}(n)} Q_g^L u_g + \sum_{i\in I(n)} Q_i v_i - \sum_{c\in C(n)} Q_c(1-x_c),$$

$$\rho_n + \phi + \sum_{f\in\mathcal{F}(\mathcal{R}_{N-1})} V_{f,n}\gamma_f = 0 \quad \forall n \in N \tag{EC.11}$$

$$\sum_{n\in N} r_n = 0 \tag{EC.12}$$

$$\sum_{n\in N} V_{f,n} r_n \leq W_f,\ \gamma_g \geq 0 \quad \forall f \in \mathcal{F}(\mathcal{R}_{N-1}) \tag{EC.13}$$

$$\sum_{g\in G^{SLOW}} K_g u_g + \sum_{i\in I} P_i Q_i v_i + \sum_{c\in C} P_c Q_c x_c + \sum_{r\in R} P_r Q_r y_r \leq$$

$$\sum_{n\in N} \rho_n \cdot \sum_{c\in C(n)} Q_c + \sum_{r\in R} Q_r \pi_r - \Bigg(\sum_{g\in G^{SLOW}} \sigma_g +$$

$$\sum_{g\in G^{FAST}} \Bigg(\sum_{i\in I(g)} \varsigma_i + \tau_g \Bigg) + \sum_{g\in G} Q_g^U \nu_g + \sum_{c\in C} \sigma_c +$$

$$\sum_{r\in R}\sigma_r + \sum_{f\in\mathcal{F}(\mathcal{R}_{N-1})} W_f\gamma_f \Bigg) \tag{EC.14}$$

The objective function (EC.7) consists of the total cost of production, demand response and reserve response. Constraints (EC.8) – (EC.10) impose the respective domains for generators, consumers and reserves. Constraints (EC.11) – (EC.13) impose network constraints and network price equilibrium. These constraints are written out in terms of the facets of the feasible set of net injections under N-1 security, $\mathcal{F}(\mathcal{R}_{N-1})$. This set corresponds to power balance and the thermal limits of lines over all N-1 transmission contingencies. Constraint (EC.14) enforces the equality of social welfare and total surplus, ensuring that European restrictions on prices are respected (see section EC.3).

Formulation (EC.7) – (EC.14) uses a quadratic number of constraints (EC.13) and variables γ_f, in the number of lines of the system, in order to define the net injection set explicitly. In order to solve (EC.7) – (EC.14) efficiently for realistic systems, we use the same algorithm as in section 3.1 with a nodal market clearing oracle ($NMCO$) that solves problem (EC.7)–(EC.14) with matrices V, W generated by the cutting-plane procedure instead of using the facets of $\mathcal{P}_{N-1}^{FB-EP}$. Starting from a loose outer approximation, each iteration of the cutting-plane procedure adds a new constraint of the type (EC.13) and re-solves the market clearing problem. Note that adding a new row to the system $Vr \leq W$ requires also adding a new variable γ associated to that row in the $NMCO$. In other words, in the presence of block bids and European pricing rules, our cutting-plane procedure becomes a column-and-constraint generation algorithm.

EC.2.1.2. Real-time market model Following Fig. EC.1, in real time the system is bound to the commitment status decided using the day-ahead market clearing model, $\bar{u}^{DA}$, for all slow generators. Additionally, the realized renewable injections and generation outages can modify the quantities offered in the real-time market Q^{RT} relative to what is offered in the day-ahead market Q. Transmission line outages modify the topology of the network, leaving only lines in $L^{RT} \subseteq L$ online in real-time operation. We model the real-time market following these changes in the power

grid as problem (EC.15) – (EC.21), where we have removed all constant quantities cleared in the day-ahead market.

$$\min_{u,v,x,f,\theta} \ \sum_{i\in I} P_i Q_i^{RT} v_i + \sum_{c\in C} P_c Q_c x_c \tag{EC.15}$$

$$\text{s.t.} \quad 0 \le u_g \le \bar{u}_g^{DA} \quad \forall g \in G^{SLOW} \tag{EC.16}$$

$$0 \le v_i \le \bar{u}_g^{DA} \quad \forall i \in I(g), g \in G^{SLOW} \tag{EC.17}$$

$$0 \le v_i \le 1 \quad \forall i \in I(g), g \in G^{FAST} \tag{EC.18}$$

$$0 \le x_c \le 1 \quad \forall c \in C \tag{EC.19}$$

$$\sum_{l\in L^{RT}(n,\cdot)} f_l - \sum_{l\in L^{RT}(\cdot,n)} f_l = \sum_{g\in G^{SLOW}(n)} Q_g^{L,RT} u_g + \sum_{i\in I(n)} Q_i^{RT} v_i - \sum_{c\in C(n)} Q_c(1-x_c) \quad \forall n \in N \quad [\rho_n] \tag{EC.20}$$

$$-F_l \le f_l \le F_l, \ f_l = B_l\left(\theta_{m(l)} - \theta_{n(l)}\right) \quad \forall l \in L^{RT} \tag{EC.21}$$

The objective function (EC.15) corresponds to real-time cost, consisting of production cost and demand response. Constraints (EC.16), (EC.17) restrict the production of slow generators according to the results of the day-ahead market. Constraints (EC.18) – (EC.21) model fast generators, consumers and the available transmission grid. Real-time energy prices are obtained as the dual of the balance constraint (EC.20) and are used in order to clear real-time quantities.

EC.2.2. Two-settlement zonal electricity market models

We model two-settlement zonal markets following Fig. EC.1, which is itself based on the existing literature (Ehrenmann and Smeers 2005). The day-ahead market is cleared using a zonal model for the grid, and system operators perform congestion management and balancing in real time.

The day-ahead models presented in this section differ from the simplified zonal models of section 2 in that (*i*) they consider the commitment decisions of slow generators and (*ii*) they consider all N-1 contingencies when determining the feasible set of zonal net positions (FBMC) or inter-zonal

exchanges (ATCMC). In order to solve the mathematical programs that ensure N-1 robustness, we employ the algorithms presented in section 3.2 for FBMC and in section EC.1.2 for ATCMC.

In what follows, we present the day-ahead models for FBMC and ATCMC, and then we introduce the real-time congestion management and balancing (CM&B) model, common for both FBMC and ATCMC.

EC.2.2.1. Day-ahead flow-based market coupling with exact projection The day-ahead market clearing problem under FBMC can be cast as the mathematical program (EC.22) – (EC.29), where we use the domains defined in (EC.3) – (EC.6) for generators, consumers and reserves.

$$\min_{\substack{u,v,w,x,y,p\\ \sigma,\varsigma,\tau,\nu,\phi,\gamma,\rho,\pi}} \quad \sum_{g\in G^{SLOW}} K_g u_g + \sum_{i\in I} P_i Q_i v_i + \sum_{c\in C} P_c Q_c x_c + \sum_{r\in R} P_r Q_r y_r \tag{EC.22}$$

$$\text{s.t.} \quad \left(u_g, v_{I(g)}, w_g, \sigma_g, \varsigma_{I(g)}, \tau_g, \nu_g, \rho_{z(g)}, \pi_{r(g)}\right) \in \mathcal{D}_g^{SLOW} \quad \forall g \in G^{SLOW},$$

$$\left(v_{I(g)}, w_g, \varsigma_{I(g)}, \tau_g, \nu_g, \rho_{z(g)}, \pi_{r(g)}\right) \in \mathcal{D}_g^{FAST} \quad \forall g \in G^{FAST} \tag{EC.23}$$

$$\left(x_c, \sigma_c, \rho_{n(c)}\right) \in \mathcal{D}_c \quad \forall c \in C \tag{EC.24}$$

$$\left(w_{G(r)}, y_r, \sigma_r, \pi_r\right) \in \mathcal{D}_r \quad \forall r \in R \tag{EC.25}$$

$$p_z = \sum_{g\in G^{SLOW}(z)} Q_g^L u_g + \sum_{i\in I(z)} Q_i v_i - \sum_{c\in C(z)} Q_c(1-x_c),$$

$$\rho_z + \phi + \sum_{f\in\mathcal{F}(\mathcal{P}_{N-1}^{FB-EP})} V_{f,z}\gamma_f = 0 \quad \forall z \in Z \tag{EC.26}$$

$$\sum_{z\in Z} p_z = 0 \tag{EC.27}$$

$$\sum_{z\in Z} V_{f,z} p_z \le W_f,\ \gamma_f \ge 0 \quad \forall f \in \mathcal{F}(\mathcal{P}_{N-1}^{FB-EP}) \tag{EC.28}$$

$$\sum_{g\in G^{SLOW}} K_g u_g + \sum_{i\in I} P_i Q_i v_i + \sum_{c\in C} P_c Q_c x_c + \sum_{r\in R} P_r Q_r y_r \le$$

$$\sum_{z\in Z} \rho_z \cdot \sum_{c\in C(z)} Q_c + \sum_{r\in R} Q_r \pi_r - \left(\sum_{g\in G^{SLOW}} \sigma_g -\right.$$

$$\sum_{g\in G^{FAST}}\left(\sum_{i\in I(g)}\varsigma_i+\tau_g\right)+\sum_{g\in G}Q_g^U\nu_g+\sum_{c\in C}\sigma_c+$$
$$\sum_{r\in R}\sigma_r+\sum_{f\in\mathcal{F}(\mathcal{P}_{N-1}^{FB-EP})}W_f\gamma_f\Bigg) \tag{EC.29}$$

The objective function (EC.22) and the constraints of generators (EC.23), consumers (EC.24) and reserves (EC.25) are analogous to those of the nodal day-ahead market clearing problem (EC.7) – (EC.14). The only difference is that we now use zonal prices instead of nodal prices for energy. Constraints (EC.26) – (EC.28) model primal and dual constraints for the zonal network model. Constraints (EC.26) define zonal net positions p_z and zonal prices ρ_z. Constraint (EC.27) enforces system-wide power balance. Constraints (EC.28) enforce that zonal net positions belong in the flow based domain $\mathcal{P}_{N-1}^{FB-EP}$, by enumerating the facets of $\mathcal{P}_{N-1}^{FB-EP}$ denoted as $\mathcal{F}(\mathcal{P}_{N-1}^{FB-EP})$. Here, we use the same definition of $\mathcal{P}_{N-1}^{FB-EP}$ as in section 3.2, ignoring the technical minimum of slow thermal generators in order to ensure that $\mathcal{P}_{N-1}^{FB-EP}$ is convex. Constraints (EC.28) also enforce non-negativity of the variables γ_f, associated with the sensitivity of the objective to each facet $f\in\mathcal{F}(\mathcal{P}_{N-1}^{FB-EP})$. Finally, constraint (EC.29) enforces equality of social welfare and total surplus, ensuring that the model produces prices that respect European pricing rules.

This formulation uses an exponential number of constraints (EC.28) and variables γ_f, in the number of zones, in order to define the flow-based domain explicitly. This is a consequence of $\mathcal{P}_{N-1}^{FB-EP}$ being a projection of all the nodal equations of the system under full availability and all N-1 conditions onto the space of zonal net positions. We solve the problem by adapting our cutting plane procedure as we do for the day-ahead nodal electricity market (see subsection EC.2.1.1). Concretely, we replace the zonal market clearing oracle $ZMCO$ by an oracle that solves (EC.22) – (EC.29) at each call.

EC.2.2.2. Day-ahead available-transfer-capacity market coupling Recall that clearing the day-ahead market using ATCMC requires two steps. Firstly, we compute ATCs by solving the mathematical program (9) – (11) with the cutting-plane algorithm described in section EC.1.2.

Then, using the computed ATCs, we clear the day-ahead energy market by solving the mathematical program (EC.30) – (EC.36), where we use (again) the domains defined in (EC.3) – (EC.6) for generators, consumers and reserves.

$$\min_{\substack{u,v,w,x,y,e\\ \sigma,\varsigma,\tau,\nu,\gamma,\rho,\pi}} \sum_{g\in G^{SLOW}} K_g u_g + \sum_{i\in I} P_i Q_i v_i + \sum_{c\in C} P_c Q_c x_c + \sum_{r\in R} P_r Q_r y_r \tag{EC.30}$$

$$\text{s.t.} \quad \left(u_g, v_{I(g)}, w_g, \sigma_g, \varsigma_{I(g)}, \tau_g, \nu_g, \rho_{z(g)}, \pi_{r(g)}\right) \in \mathcal{D}_g^{SLOW} \quad \forall g \in G^{SLOW},$$

$$\left(v_{I(g)}, w_g, \varsigma_{I(g)}, \tau_g, \nu_g, \rho_{z(g)}, \pi_{r(g)}\right) \in \mathcal{D}_g^{FAST} \quad \forall g \in G^{FAST} \tag{EC.31}$$

$$\left(x_c, \sigma_c, \rho_{n(c)}\right) \in \mathcal{D}_c \quad \forall c \in C \tag{EC.32}$$

$$\left(w_{G(r)}, y_r, \sigma_r, \pi_r\right) \in \mathcal{D}_r \quad \forall r \in R \tag{EC.33}$$

$$\sum_{t\in T(z,\cdot)} e_t - \sum_{t\in T(\cdot,z)} e_t = \sum_{g\in G^{SLOW}(z)} Q_g^L u_g + \sum_{i\in I(z)} Q_i v_i - \sum_{c\in C(z)} Q_c(1-x_c) \quad \forall z \in Z \tag{EC.34}$$

$$-ATC_t^- \le e_t \le ATC_t^+,\ \gamma_t^- \ge 0,\ \gamma_t^+ \ge 0,$$

$$\gamma_t^+ - \gamma_t^- = \rho_{b(t)} - \rho_{a(t)} \quad \forall t \in T \tag{EC.35}$$

$$\sum_{g\in G^{SLOW}} K_g u_g + \sum_{i\in I} P_i Q_i v_i + \sum_{c\in C} P_c Q_c x_c + \sum_{r\in R} P_r Q_r y_r \le \sum_{z\in Z} \rho_z \cdot \sum_{c\in C(z)} Q_c + \sum_{r\in R} Q_r \pi_r - \left(\sum_{g\in G^{SLOW}} \sigma_g - \sum_{g\in G^{FAST}} \left(\sum_{i\in I(g)} \varsigma_i + \tau_g \right) + \sum_{g\in G} Q_g^U \nu_g + \sum_{c\in C} \sigma_c + \sum_{r\in R} \sigma_r + \sum_{t\in T} \left(ATC_t^+ \gamma_t^+ + ATC_t^- \gamma_t^- \right) \right) \tag{EC.36}$$

The objective function (EC.30) and constraints (EC.31) – (EC.33) are identical to those of the FBMC day-ahead clearing model (EC.22) – (EC.29). Constraints (EC.34), (EC.35) enforce primal and dual constraints over the transportation network between zones, with exchanges through interconnectors limited by the ATCs. Constraints (EC.36) enforce strong duality between the primal and dual parts of the clearing problem, thereby, ensuring that ρ^* are supporting prices of the clearing decisions.

EC.2.2.3. Real-time congestion management and balancing We model real-time congestion management and balancing as the mathematical program (EC.37) – (EC.38).

$$\min_{u,v,x,f,\theta,p} \sum_{i\in I} P_i Q_i^{RT} v_i + \sum_{c\in C} P_c Q_c x_c + \sum_{z\in Z} \hat{P} \left| p_z - \bar{p}_z^{DA} \right| \tag{EC.37}$$

$$\text{s.t.} \quad (\text{EC.16}) - (\text{EC.21}) \tag{EC.38}$$

$$p_z = \sum_{g\in G^{SLOW}(z)} Q_g^{L,RT} u_g + \sum_{i\in I(z)} Q_i^{RT} v_i - \sum_{c\in C(z)} Q_c(1-x_c) \quad \forall z \in Z \tag{EC.39}$$

This problem is essentially the same as (EC.15) – (EC.21). The only difference in terms of modeling is that, in (EC.37), we penalize deviations from day-ahead net positions $\bar{p}^{DA}$ at $\hat{P} := \max_{i\in I} P_i$. The goal is to account for the restriction that market participants within each zone must remain in balance in real time, Regulation (EU) 2017/2195, while maintaining feasibility of the real-time model. On the other hand, there is an important difference with (EC.15) – (EC.21) in terms of pricing: in (EC.37) – (EC.38) real-time quantities are paid-as-bid (ACER and CEER 2017), instead of using locational marginal prices.

EC.3. Derivation of day-ahead electricity market models with strict linear pricing

The presence of binary commitment variables in day-ahead electricity market models renders the derivation of prices for these markets a non-trivial task. Equilibrium prices, in the presence of integer decision variables, may not exist, depending on the parameters of the market clearing problem at hand, see Vohra (2011). This can lead to (*i*) paradoxically accepted bids, i.e. bids that are accepted at a loss for the bidding participant, and (*ii*) paradoxically rejected bids, i.e. rejected bids that if accepted would generate a profit for the bidding participant. Paradoxically rejected block bids are allowed and not compensated in most electricity markets (EPEX Spot et al. 2016), (FERC 2014). The treatment of paradoxically accepted bids, on the other hand, differs among markets: U.S. markets allow paradoxically accepted bids and cover the losses of bidding participants through uplift payments (FERC 2014), while European markets do not allow paradoxically accepted bids (EPEX Spot et al. 2016).

In the following we derive a model for the nodal day-ahead market clearing problem respecting the European pricing restrictions, following the mixed-integer linear programming framework of Madani and Van Vyve (2015). We start by expressing the unit commitment problem in terms of continuous bids, block bids and linked families, (EC.40) – (EC.53).

$$\min_{u,v,w,x,y,r} \sum_{g\in G^{SLOW}} K_g u_g + \sum_{i\in I} P_i Q_i v_i + \sum_{c\in C} P_c Q_c x_c + \sum_{r\in R} P_r Q_r y_r \tag{EC.40}$$

$$\text{s.t.} \quad u_g \le 1 \qquad \forall g \in G \quad [\sigma_g] \tag{EC.41}$$

$$v_i \le u_{g(i)} \qquad \forall i \in I \quad [\varsigma_i] \tag{EC.42}$$

$$w_g \le u_g \qquad \forall g \in G^{SLOW} \quad [\tau_g] \tag{EC.43}$$

$$w_g \le 1 \qquad \forall g \in G^{FAST} \quad [\tau_g] \tag{EC.44}$$

$$Q_g^L u_g + \sum_{i\in I(g)} Q_i v_i + Q_g^R w_g \le Q_g^U \qquad \forall g \in G^{SLOW} \quad [\nu_g] \tag{EC.45}$$

$$\sum_{i\in I(g)} Q_i v_i + Q_g^R w_g \le Q_g^U \qquad \forall g \in G^{FAST} \quad [\nu_g] \tag{EC.46}$$

$$x_c \le 1 \qquad \forall c \in C \quad [\sigma_c] \tag{EC.47}$$

$$r_n = \sum_{g\in G(n)} Q^L u_g + \sum_{i\in I(n)} Q_i v_i - \sum_{c\in C(n)} Q_c (1 - x_c) \qquad \forall n \in N \quad [\rho_n] \tag{EC.48}$$

$$\sum_{n\in N} r_n = 0 \qquad [\phi] \tag{EC.49}$$

$$\sum_{n\in N} V_{f,n} r_n \le W_f \qquad \forall f \in \mathcal{F}(\mathcal{R}_{N-1}) \quad [\gamma_f] \tag{EC.50}$$

$$y_r \le 1 \qquad \forall r \in R \quad [\sigma_r] \tag{EC.51}$$

$$Q_r (1 - y_r) - \sum_{g\in G(r)} Q_g^R w_g \le 0 \qquad \forall r \in R \quad [\pi_a] \tag{EC.52}$$

$$u, v, w, x, y \ge 0, \; u_g \in \{0, 1\} \; \forall g \in G \tag{EC.53}$$

The objective function (EC.53) corresponds to the total cost of operation. This includes production, demand response and reserve response costs. Constraints (EC.41) – (EC.46) impose that production and reserve bids can be accepted at most once, and that the total capacity of each

generator must be respected. Constraints (EC.47) – (EC.52) enforce limits on demand response bids, nodal power balance, and transmission constraints under N-1 security and reserve requirements. Using the dual variables indicated in brackets beside each constraint, we can write the Karush-Kuhn-Tucker conditions of the linear relaxation of (EC.40) – (EC.53) as follows:

$$0 \leq \sigma_g \perp u_g - 1 \leq 0 \quad \forall g \in G^{SLOW} \tag{EC.54}$$

$$0 \leq \varsigma_i \perp v_i - u_g \leq 0 \quad \forall g \in G^{SLOW}, i \in I(g) \tag{EC.55}$$

$$0 \leq \tau_g \perp w_g - u_g \leq 0 \quad \forall g \in G^{SLOW} \tag{EC.56}$$

$$0 \leq \nu_g \perp Q_g^L u_g + \sum_{i \in I(g)} Q_i v_i + Q_g^R w_g - Q_g^U \leq 0 \quad \forall g \in G^{SLOW} \tag{EC.57}$$

$$0 \leq \varsigma_i \perp v_i - 1 \leq 0 \quad \forall g \in G^{FAST}, i \in I(g) \tag{EC.58}$$

$$0 \leq \tau_g \perp w_g - 1 \leq 0 \quad \forall g \in G^{FAST} \tag{EC.59}$$

$$0 \leq \nu_g \perp \sum_{i \in I(g)} Q_i v_i + Q_g^R w_g - Q_g^U \leq 0 \quad \forall g \in G^{FAST} \tag{EC.60}$$

$$0 \leq \sigma_c \perp x_c - 1 \leq 0 \quad \forall c \in C \tag{EC.61}$$

$$\rho_n \perp r_n - \sum_{g \in G^{SLOW}(n)} Q_g^L u_g - \sum_{i \in I(n)} Q_i v_i + \sum_{c \in C(n)} Q_c (1 - x_c) = 0 \quad \forall n \in N \tag{EC.62}$$

$$\phi \perp \sum_{n \in N} r_n = 0 \tag{EC.63}$$

$$0 \leq \gamma_f \perp \sum_{n \in N} V_{f,n} r_n - W_f \leq 0 \quad \forall f \in \mathcal{F}(\mathcal{R}_{n-1}) \tag{EC.64}$$

$$0 \leq \sigma_r \perp y_r - 1 \leq 0 \quad \forall r \in R \tag{EC.65}$$

$$0 \leq \pi_r \perp Q_r (1 - y_r) - \sum_{g \in G(r)} Q_g^R w_g \leq 0 \quad \forall r \in R \tag{EC.66}$$

$$0 \leq u_g \perp \sigma_g - \sum_{i \in I(g)} \varsigma_i - \tau_g + Q_g^L \nu_g - Q_g^L \rho_{n(g)} + K_g \geq 0 \quad \forall g \in G^{SLOW} \tag{EC.67}$$

$$0 \leq v_i \perp \varsigma_i + Q_i \nu_{g(i)} - Q_i \rho_{n(i)} + Q_i P_i \geq 0 \quad \forall i \in I \tag{EC.68}$$

$$0 \leq w_g \perp \tau_g + Q_g^R \nu_g - Q_g^R \pi_{r(g)} \geq 0 \quad \forall g \in G \tag{EC.69}$$

$$0 \leq x_c \perp \sigma_c - Q_c \rho_{n(c)} + Q_c P_c \geq 0 \quad \forall c \in C \tag{EC.70}$$

$$r_n \perp \rho_n + \phi + \sum_{f \in \mathcal{F}(\mathcal{R}_{N-1})} V_{f,n} \gamma_f = 0 \quad \forall n \in N \tag{EC.71}$$

$$0 \leq y_r \perp \sigma_r - Q_r \pi_r + Q_r P_r \geq 0 \quad \forall r \in R. \tag{EC.72}$$

These complementarity conditions guarantee the existence of equilibrium prices for energy and reserve, $\boldsymbol{\rho}^*$ and $\boldsymbol{\pi}^*$, for the relaxed market clearing problem. A direct consequence of this result is that if the solution set of the linear relaxation of (EC.40) – (EC.53) contains a binary $\boldsymbol{u}$, then $\boldsymbol{\rho}^*$ and $\boldsymbol{\pi}^*$ are also equilibrium prices for the original clearing problem. On the other hand, imposing integrality of $\boldsymbol{u}$ along with (EC.54) – (EC.72) can result in an infeasible system of equations.

While a complete description of the consequences of complementarity system (EC.54) – (EC.72) is out of the scope of this chapter, it is important to present these consequences for $\boldsymbol{u}$ in order to understand how to relax the complementarity system so that it remains feasible when integrality constraints are included in the market clearing model. For any slow generator $g \in G^{SLOW}$, if its overall surplus σ_g is positive, then by constraint (EC.54) it must be the case that $u_g = 1$ (in-the-money bids must be accepted). On the other hand, if $\sigma_g = 0$ and the right side of (EC.67) does not hold with equality, then $u_g = 0$ (out-of-the-money bids must be rejected). Additionally, according to (EC.67), child bids in $I(g)$ and reserves can pass surplus to their parent. This allows u_g to be 1 even when $\rho_{n(g)} Q_g^L - K_g < 0$.

If the complementarity restriction of (EC.54) is relaxed, one can paradoxically reject any linked bid family submitted by a slow generator. This is in line with the principles of the European market (EPEX Spot et al. 2016, Madani and Van Vyve 2015). Furthermore, we can guarantee the feasibility of the complementarity system with integrality constrains, independently of the parameters of the bids submitted by market participants. We formalize the latter result in the following proposition.

Proposition EC.4. *Assume that $W_f \geq 0 \ \forall f \in \mathcal{F}(\mathcal{R}_{N-1})$. Then, the system* (EC.54) – (EC.72)*, with complementarity relaxed for* (EC.54) *and binary restrictions on u, is feasible.*

Proof of Proposition EC.4 First, note that problem (EC.40) – (EC.53) is feasible since, due to our assumption, $u=0, v=0, w=0, x=1, y=1, r=0$ is a feasible point. Further, let $(v^*_{u=0}, w^*_{u=0}, x^*_{u=0}, y^*_{u=0}, r^*_{u=0})$ be an optimal solution for the remaining linear program after fixing $u=0$ in (EC.40) – (EC.53). We claim that there exist values $(\bar{\sigma}, \bar{\varsigma}, \bar{\tau}, \bar{\nu}, \bar{\rho}, \bar{\phi}, \bar{\gamma}, \bar{\pi})$ such that $(v^*_{u=0}, w^*_{u=0}, x^*_{u=0}, y^*_{u=0}, r^*_{u=0}, \bar{\sigma}, \bar{\varsigma}, \bar{\tau}, \bar{\nu}, \bar{\rho}, \bar{\phi}, \bar{\gamma}, \bar{\pi})$ is feasible for (EC.54) – (EC.72), with complementarity relaxed for (EC.54).

Indeed, we can set $\bar{\nu}_g := 0$ and $\bar{\tau}_g, \bar{\varsigma}_i \ \forall i \in I(g), \bar{\sigma}_g$ to arbitrarily large values for all $g \in G^{SLOW}$, so that constraints (EC.67), (EC.68) and (EC.69) become redundant for all linked bid families. The remaining complementarity system coincides with the Karush-Kuhn-Tucker conditions of (EC.40) – (EC.53) after fixing $\boldsymbol{u}=0$, which by feasibility of (EC.40) – (EC.53), we know has at least one feasible solution. □

Note that the assumption adopted in Prop. EC.4 is not restrictive for real networks, since it is equivalent to assuming that transmission lines have a non-negative capacity.

Using the previous observations, we can formulate the nodal day-ahead market clearing model with pricing restrictions as the mathematical program with complementarity constraints (MPCC) (EC.73) – (EC.75), which is reformulated as a mixed-integer linear program in Prop. EC.5. The reformulation is exressed as follows.

$$\min_{\substack{u,v,w,x,y,r \\ \sigma,\varsigma,\tau,\nu,\rho,\phi,\gamma,\pi}} \quad \sum_{g \in G^{SLOW}} K_g u_g + \sum_{i \in I} P_i Q_i v_i + \sum_{c \in C} P_c Q_c x_c + \sum_{r \in R} P_r Q_r y_r \tag{EC.73}$$

$$\text{s.t.} \quad 0 \le \sigma_g, \ u_g \in \{0,1\} \quad \forall g \in G^{SLOW} \tag{EC.74}$$

$$(\text{EC.55}) - (\text{EC.72}) \tag{EC.75}$$

Proposition EC.5. *Problem* (EC.73) – (EC.75) *and problem* (EC.7) – (EC.14) *are equivalent in the following sense:*

1. *for each feasible point* $(u, v, w, x, y, r, \sigma, \varsigma, \tau, \nu, \rho, \phi, \gamma, \pi)$ *of* (EC.73) – (EC.75)*, there exists* $\tilde{\sigma}$ *such that* $(u, v, w, x, y, r, \tilde{\sigma}, \varsigma, \tau, \nu, \rho, \phi, \gamma, \pi)$ *is feasible for* (EC.7) – (EC.14).

2. *Conversely, for each feasible point* $(u, v, w, x, y, r, \sigma, \varsigma, \tau, \nu, \rho, \phi, \gamma, \pi)$ *of* (EC.7) – (EC.14)*, there exists* $\tilde{\sigma}$ *such that* $(u, v, w, x, y, r, \tilde{\sigma}, \varsigma, \tau, \nu, \rho, \phi, \gamma, \pi)$ *is feasible for* (EC.73) – (EC.75)*.*

Proof of Proposition EC.5 Analogous to proof of Theorem 2 of Madani and Van Vyve (2015). □

The procedure applied in this section for obtaining a mixed-integer linear programming formulation for the nodal day-ahead market clearing problem that respects European pricing restrictions consists of three main steps: (*i*) writing the Karush-Kuhn-Tucker conditions, (*ii*) developing a modified version of the dual constraints that admits paradoxical rejection of linked families, and (*iii*) enforcing these dual constraints alongside primal constraints. We apply the same procedure to zonal day-ahead market clearing models, obtaining the formulation (EC.22) – (EC.29) for flow-based market coupling and the formulation (EC.30) – (EC.36) for available-transfer-capacity market coupling.

EC.4. Implementation and simulation details

Our case study corresponds to the CWE instance of Aravena and Papavasiliou (2017) with the following modifications: we remove Switzerland, since it is not part of the current implementation of FBMC, and we add (*i*) forced outage rates for thermal generators based on NERC (2016), (*ii*) cost of CO_2 emissions, with emission rates derived from Moomaw et al. (2011) and valued at the average intra-day price of emissions in 2013-2017 (EEX AG 2018), (*iii*) forced outage rates for transmission lines from Ekisheva and Gugel (2015) and (*iv*) existing phase shifters at the borders of Belgium.

We implement the models and algorithms involved in simulating LMP, FBMC and ATCMC (presented in sections EC.2, 3.2 and EC.1.2) in Julia 0.6.0 (Bezanson et al. 2017), using JuMP 0.18.0 (Dunning et al. 2017), to define the required mathematical programs. We use Gurobi 8.0.0 to solve the mixed-integer linear programs for day-ahead market clearing and Ipopt 3.12.8 (Wächter and Biegler 2006), compiled with Coin-HSL (HSL 2015), for the computation of volume-maximizing ATCs. We use Xpress 8.5.0 for solving the linear programs that simulate real-time operations.

We deploy our algorithms on high-performance computing clusters, using the built-in message passing implementation of Julia. We parallelize the simulation over different snapshots of operation. We used the Cab cluster, hosted at the Lawrence Livermore National Laboratory and the Lemaitre2 cluster, hosted at the Université catholique de Louvain (UCLouvain), for development runs of the models. We used the Lemaitre3 cluster, also hosted at UCLouvain, for the final run, which consumed 7 579 core-hours.

The analysis of the results is performed using Julia and R (R Core Team 2015). We use arithmetic averages to aggregate results across snapshots and median centers (Gower 1974), in order to aggregate results across realizations of uncertainty. We use the median center in order to remove the effect of low-probability events from central tendency indicators.

References

ACER, CEER (2017) Annual report on the results of monitoring the internal electricity and gas markets in 2016.

Benders JF (1962) Partitioning procedures for solving mixed-variables programming problems. *Numerische Mathematik* 4(1):238–252, ISSN 0945-3245, URL http://dx.doi.org/10.1007/BF01386316.

Bezanson J, Edelman A, Karpinski S, Shah VB (2017) Julia: A fresh approach to numerical computing. *SIAM Review* 59(1):65–98, URL http://dx.doi.org/10.1137/141000671.

Dunning I, Huchette J, Lubin M (2017) JuMP: A modeling language for mathematical optimization. *SIAM Review* 59(2):295–320, URL http://dx.doi.org/10.1137/15M1020575.

EEX AG (2018) European Emission Allowances. URL https://www.eex.com/en/market-data/environmental-markets/spot-market/european-emission-allowances, accessed: 2018-02-14.

Ekisheva S, Gugel H (2015) North American AC circuit outage rates and durations in assessment of transmission system reliability and availability. *2015 IEEE Power Energy Society General Meeting*, 1–5, ISSN 1932-5517, URL http://dx.doi.org/10.1109/PESGM.2015.7285782.

EPEX Spot, GME, Noord Pool, OMIE, OPCOM, OTE, TGE (2016) EUPHEMIA Public Description.

Federal Energy Regulatory Commission (FERC) (2007) Initial Decision, Docket No. EL03-180-000.

Federal Energy Regulatory Commission (FERC) (2014) Uplift in RTO and ISO markets.

Gower JC (1974) Algorithm AS 78: The mediancentre. *Journal of the Royal Statistical Society. Series C (Applied Statistics)* 23(3):466–470, URL http://www.jstor.org/stable/2347150.

HSL (2015) A collection of fortran codes for large scale scientific computation. URL http://www.hsl.rl.ac.uk/.

Kamat R, Oren SS (2002) Multi-settlement systems for electricity markets: zonal aggregation under network uncertainty and market power. *Proceedings of the 35th Annual Hawaii International Conference on System Sciences*, 739–748, URL http://dx.doi.org/10.1109/HICSS.2002.993956.

Kamat R, Oren SS (2004) Two-settlement systems for electricity markets under network uncertainty and market power. *Journal of Regulatory Economics* 25(1):5–37, ISSN 1573-0468, URL http://dx.doi.org/10.1023/B:REGE.0000008653.08554.81.

Madani M, Van Vyve M (2015) Computationally efficient MIP formulation and algorithms for european day-ahead electricity market auctions. *European Journal of Operational Research* 242(2):580 – 593, ISSN 0377-2217.

Moomaw W, Burgherr P, Heath G, Lenzen M, Nyboer J, Verbruggen A (2011) Annex II: Methodology. Edenhofer O, Pichs-Madruga R, Sokona Y, Seyboth K, Matschoss P, Kadner S, Zwickel T, Eickemeier P, Hansen G, Schlömer S, von Stechow C, eds., *IPCC Special Report on Renewable Energy Sources and Climate Change Mitigation* (Cambridge, United Kingdom: Cambridge University Press).

North American Electric Reliability Corporation (NERC) (2016) Generating availability data system (GADS). URL http://www.nerc.com/pa/RAPA/gads/Pages/Reports.aspx.

R Core Team (2015) *R: A Language and Environment for Statistical Computing*. R Foundation for Statistical Computing, Vienna, Austria, URL https://www.R-project.org/.

Vohra RV (2011) *Mechanism Design: A Linear Programming Approach* (Cambridge University Press), URL http://dx.doi.org/10.1017/CBO9780511835216.

Wächter A, Biegler LT (2006) On the implementation of an interior-point filter line-search algorithm for large-scale nonlinear programming. *Mathematical Programming* 106(1):25–57, ISSN 1436-4646, URL http://dx.doi.org/10.1007/s10107-004-0559-y.

Waniek D, Rehtanz C, Handschin E (2009) Analysis of market coupling based on a combined network and market model. *2009 IEEE Bucharest PowerTech*, 1–6, URL http://dx.doi.org/10.1109/PTC.2009.5282231.

Acknowledgments

The authors would like to thank Mr. Alain Marien (CREG) and Dr. Gauthier de Maere d'Aertrycke (ENGIE) for their helpful comments and discussions during the development of this work.

The authors would also like to thank Gurobi and FICO for providing distributed academic licenses for Gurobi and Xpress, respectively, the Lawrence Livermore National Laboratory for providing computing time at the Cab cluster and the Consortium des Équipements de Calcul Intensif (CÉCI) for providing computing time at the Lemaitre2 cluster.

This research was partially funded by the ENGIE Chair on Energy Economics and Energy Risk Management, the Univeristé catholique de Louvain through an FSR grant, the Bauchau Prize 2017 and the U.S. Department of Energy through the Lawrence Livermore National Laboratory under contract DE-AC52-07NA27344.